Time-Varying Expectation Effects of Switching Financial Uncertainty*

Yoosoon Chang †
Department of Economics
Indiana University

Hwagyun Kim ‡
Mays Business School
Texas A&M University

Shi Qiu §
School of Economics
Fudan University

November 18, 2021

Abstract

This paper investigates the effects of dynamic capital market conditions in a general equilibrium model, employing a process of switching steady-state levels of the volatility of market condition (SS-uncertainty). Decision-makers predict SS-uncertainty regimes using past fundamental shocks, but an exogenous uncertainty shock still exists. Model estimation uncovers evidence of state-dependent uncertainty effects. Shock responses significantly vary, depending on the current uncertainty regime and shock magnitude. In the high (low) SS-uncertainty regime, economic activities decrease (increase) regardless of shock direction. This anomaly disappears for sufficiently large uncertainty shocks. Quantitatively, a pessimistic shock produces inertia, whereas an optimistic shock boosts economic activities.

JEL Classification: E32, E44, C11

Keywords: DSGE, uncertainty, financial friction, expectation, endogenous regime switching

*We are grateful to Jack Favilukis, Ippei Fujiwara, Brigitte Hochmuth, Shane Johnson, Junior Maih, Joon Y. Park and Fei Tan for helpful discussions, and also to the participants in 2021 IAAE, 2021 RCEA Money, Macro & Finance Conference, 2021 Women in Macro, Finance and Economic History Workshop, 2020 Marleau Lecture on Economic and Monetary Policy at University of Ottawa, 2019 SETA, 2019 CEF and Keio University for their useful comments.

†Bloomington, IN 47405-7104. E-mail: yoosoon@indiana.edu.

‡College Station, TX 77843-4218. E-mail:hkim@mays.tamu.edu.

§Shanghai, China, 200433. E-mail: shiqiu@fudan.edu.cn.

1 Introduction

In this paper, we model and estimate financial uncertainty by introducing two-state regimes for the steady states of a volatility process related to capital market conditions that affect entrepreneurial activities under a dynamic stochastic general equilibrium (DSGE) framework. We label the steady state of volatility as SS-uncertainty, and our model introduces a shock to the SS-uncertainty regimes and allows transition probabilities of the regimes to vary dependent upon a set of previous shocks as well as the SS-uncertainty shock. We view that transition probabilities in our setup may characterize the (subjective) outlook on economic and financial conditions. Extending Christiano et al. (2014) (CMR), we define an uncertainty process (σ) to follow an autoregressive process

$$\log(\sigma_t/\sigma_*) \quad = \quad \rho_\sigma \log(\sigma_{t-1}/\sigma_*) + \sigma_{e,\sigma} e^*_{\sigma_t},$$

where $e^*_{\sigma_t}$ refers to a σ-shock perceived by an agent. Our main departure from CMR lies in the assumption that $e^*_{\sigma_t}$ consists of a fundamental volatility shock ($e_{\sigma,t}$) and an uncertainty shock ($\mathcal{U}_t$) associated with the economic agents' perception about steady state uncertainty. A simple example would be $e^*_{\sigma_t} = e_{\sigma_t} + \mathcal{U}_t$. An uncertainty shock $\mathcal{U}_t$ can be interpreted as a belief term resulting from processing available information, which we illustrate below. In describing an economic situation, it is customary to use two regimes, such as high and low, positive and negative, favorable and adverse, or optimistic and pessimistic. Information processing can be costly and therefore distinguishing individual economic states is difficult, especially if economic agents need to solve a highly complex multivariate optimization problem. In this vein, we suppose that the agent views that the steady state level of uncertainty can be either high ($\overline{\sigma}_{ss}$) or low ($\underline{\sigma}_{ss}$) to reflect the struggling agents' heuristic belief formation ($\overline{\sigma}_{ss} > \underline{\sigma}_{ss} > 0$). Specifically, we may express the uncertainty shock ($\mathcal{U}_t$) as

$$\mathcal{U}_t = \begin{cases} \frac{1}{\sigma_{e,\sigma}} \left[\log(\overline{\sigma}_{ss}/\sigma_*) - \rho_\sigma \log(\sigma_{ss,t-1}/\sigma_*)\right], & \text{if perceived uncertainty is high,} \\ \frac{1}{\sigma_{e,\sigma}} \left[\log(\underline{\sigma}_{ss}/\sigma_*) - \rho_\sigma \log(\sigma_{ss,t-1}/\sigma_*)\right], & \text{if otherwise.} \end{cases}$$

Combining the above two equations, we write the perception-adjusted uncertainty

process as

$$\log(\sigma_{\omega,t}/\sigma_{ss,t}) \quad = \quad \rho_\sigma \log(\sigma_{\omega,t-1}/\sigma_{ss,t-1}) + \sigma_{e,\sigma_\omega} e_{\sigma_\omega,t},$$

where $\sigma_{ss,t} = \overline{\sigma}_{ss}$ if the steady-state uncertainty is high, and $\sigma_{ss,t} = \underline{\sigma}_{ss}$, otherwise. Then, we can make the switching of $\sigma_{ss,t}$ endogenous and conditional on key economic shocks to model financial market uncertainty.

Mounting empirical evidence indicates that adverse changes in financial market conditions are among the leading sources of the sharp contraction and slow recovery of the U.S. economy during the Great Recession and its aftermath.Theoretical justifications exist as well. Cagetti et al. (2002) and Hansen (2007) show the roles of uncertainty produced by hidden Markov switching models to study equity premiums. Kim et al. (2009), Kim and Park (2018), and Kim et al. (2020) show that regime-switching models or similar nonlinear volatility models imply that the volatility of volatility is much higher in times of switching regimes or fast transitions in states. This can produce uncertainty distinct from risk. To be specific, define $X_t^\sigma = \ln \frac{\sigma_t}{\sigma_{ss,t}}$, where $X_t^\sigma = \rho X_{t-1}^\sigma + \sigma_{e,\sigma} e_{\sigma,t}$. Then, we can easily see that $\sigma_t = \exp(X_t^\sigma)\sigma_{ss,t}$, where $\sigma_{ss,t}$ is a step function having values of either $\overline{\sigma}_{ss}$ or $\underline{\sigma}_{ss}$ depending upon economic states. Taken together, our volatility process is a two-factor nonlinear model in which one factor (σ_{ss}) represents a source of uncertainty related to the economic agent's belief formation. Furthermore, because (σ_{ss}) process switches over time, X, or the logarithmic deviation of volatility from its steady state will depend on the level and change of the uncertainty regime.

Anecdotally, regime-switching frictions appear necessary to explain data, which shows significant and recurrent up-and-down variations in the corporate bond spread defined by Baa-rated bond yields over 10-year treasury rates. The spread rises in recessions and declines in expansions, where rises are associated with tightening and declines with loosening in credit conditions. Many authors (e.g., Reinhart and Rogoff (2008)) document that credit conditions drastically loosened leading up to the financial crisis. In this light, we estimate the risk and uncertainty process from the core model of CMR,[1] and demonstrates that a model without time-varying financial

[1]The uncertainty process is generated with a smoothing filter at the posterior mean. Compared to CMR, we assume away term structure, news shocks, and all distortionary taxation. The data set contains eight standard macro variables and three financial variables spanning from 1995Q1 to

Figure 1: Credit Spread, Credit Information Uncertainty and Financial Risks

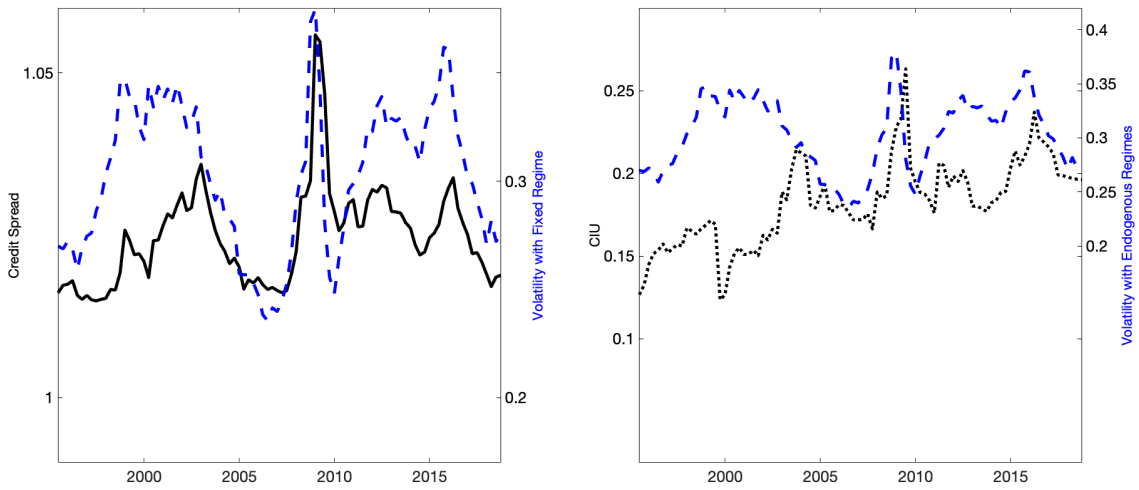

Notes: This figure compares credit spread and a credit information uncertainty measure with the volatility of capital efficiency shock, estimated without regime-switching in steady-state levels of uncertainty. The dashed blue curve (right scale) in both panels plots smoothed uncertainty (volatility) in natural log produced at the posterior mean of the estimated quantitative model with financial friction in a fixed regime, following Christiano et al. (2014). The data spans from 1995Q1 to 2018Q2. The dark curve (left scale) in the left panel plots credit spread in natural log defined by the spread of Baa-rated corporate bonds yields over U.S. 10-year constant maturity treasury rates. The dark dotted curve (left scale) in the right panel plots the issue-amount weighted credit rating dispersion (credit information uncertainty: CIU). The correlation between the credit spread and the estimated volatility (left panel) is 0.576, and the correlation between the CIU and the estimated volatility (right panel) is 0.119.

uncertainty regimes cannot fully explain the spread dynamics.

Further, we measure credit information uncertainty (CIU) as a proxy for the quantity of uncertainty, extending Kim et al. (2018) and Johnson et al. (2020) by aggregating the cross-sectional dispersion of credit ratings of firms with issue-amount weights. We believe that the CIU measure matches the description of our uncertainty term generated by the cross-sectional volatility of "perceived" market conditions.

2018Q2 and is inherently a subset of CMR. CMR reports a similar comparison in Panel F of Figure 1.

Figure 2: Credit spread, Credit Information Uncertainty, and Financial Risk and Uncertainty

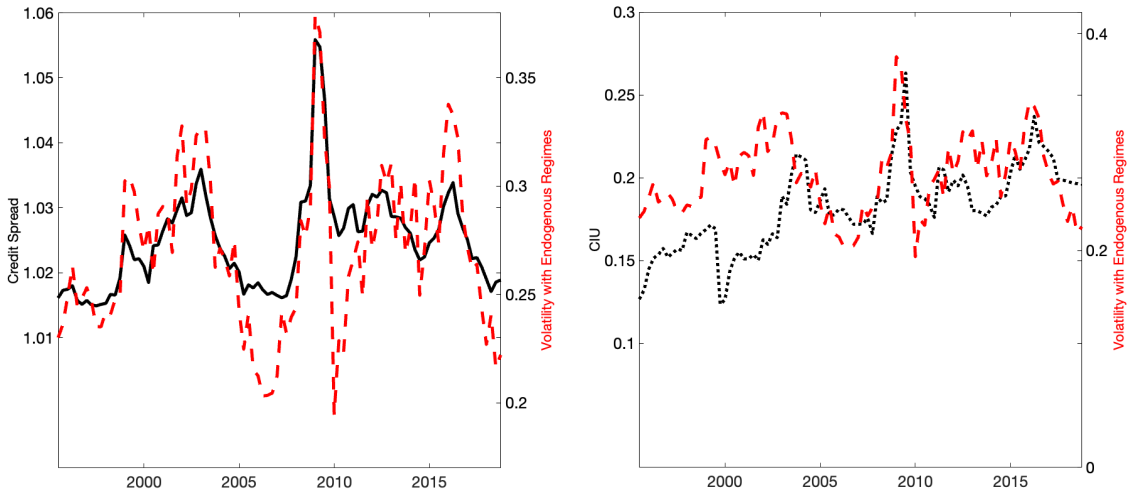

Notes: This figure compares credit spread and a credit information uncertainty measure with the volatility of capital efficiency shock, estimated with endogenous regime-switching in steady-state levels of uncertainty. The dashed red curve (right scale) in both panels plots smoothed risk and uncertainty (volatility) in natural log produced at the posterior mean of the estimated quantitative model with financial friction with the endogenous regime-switching mechanism suggested in Chang et al. (2017). The data spans from 1995Q1 to 2018Q2. The dark curve (left scale) in the left panel plots credit spread in natural log defined by the spread of Baa-rated corporate bonds yields over U.S. 10-year constant maturity treasury rates. The dark dotted curve (left scale) in the right panel plots the issue-amount weighted credit rating dispersion (credit information uncertainty: CIU). The correlation between the credit spread and the estimated volatility (left panel) is 0.792, and the correlation between the CIU and the estimated volatility (right panel) is 0.325.

We compare this credit uncertainty proxy with the estimated volatility process without regime-switching, again to find that the conventional fixed regime model has limitations in measuring uncertainty. Figure 1 suggests that the estimated model under a fixed financial condition regime reveals two major episodes of disconnect between credit spreads and uncertainty in the period of 1995-early 2000, and the period since 2010, where the model overstates the level of uncertainty by a significant margin. A similar pattern prevails between the estimated risk process and the credit information uncertainty in that the estimated risk process misses important fluctuations of the CIU.

Figure 3: Credit spread, Credit Information Uncertainty, and Financial Uncertainty

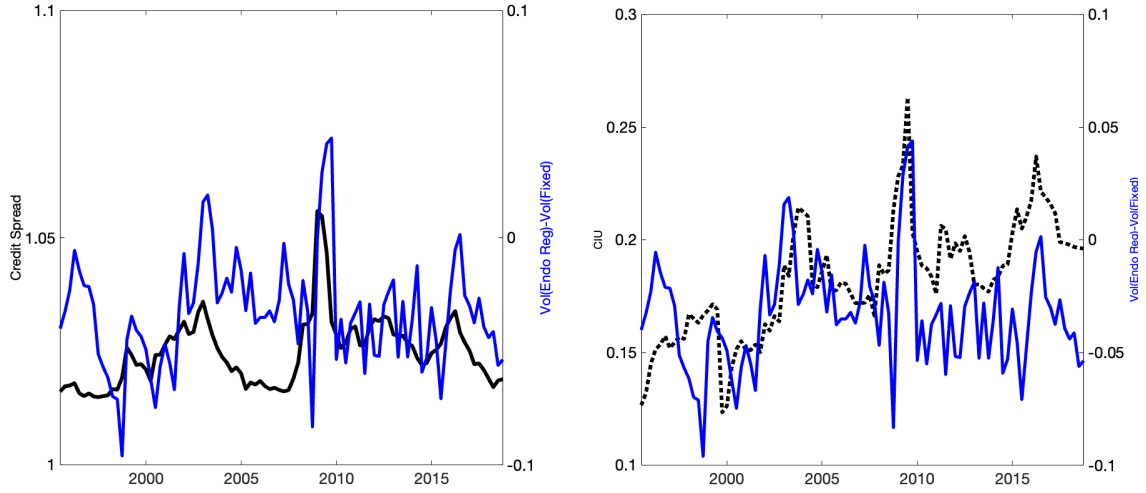

Notes: This figure compares credit spread and a credit information uncertainty measure with the differences of capital efficiency volatilities estimated with and without regime-switching in the steady-state level of uncertainty. The volatility difference is to identify financial uncertainty arising from endogenous regime-switching. The solid blue curve (right scale) in both panels plots smoothed uncertainty (volatility difference) in natural log produced at the posterior mean of the estimated quantitative model with and without the endogenous regime-switching mechanism suggested in Chang et al. (2017). The data spans from 1995Q1 to 2018Q2. The dark curve (left scale) in the left panel plots credit spread in natural log defined by the spread of Baa-rated corporate bonds yields over U.S. 10-year constant maturity treasury rates. The dark dotted curve (left scale) in the right panel plots the issue-amount weighted credit rating dispersion (credit information uncertainty: CIU). The correlation between the credit spread and the estimated volatility difference (left panel) is 0.40, and the correlation between the CIU and the estimated volatility difference (right panel) is 0.328.

A potential answer to the slow rebound rate lies in uncertainty and the related agents' expectations. With a bleak outlook of financial conditions, agents substitute out future investment for current investment since the price of credit appears expensive going forward, resulting in slower future growth and the resultant low credit spreads reflecting the lower credit demand. Regarding credit information uncertainty, uncertainty may be lower when an economy is already in a bad state because of the lower likelihood of a sudden regime change to a good state. Thus, transitions in regimes amplify uncertainty effect, and when the economy is stable, whether in a

good or a bad state, the uncertainty effect can be less intense. A proper adjustment deems necessary due to this nonlinear and non-monotonic uncertainty link.

Our uncertainty-augmented expectation channel show some promising results. For instance, Figure 2 plots the comparison results when the volatility of capital efficiency shock is estimated using the endogenous regime-switching model applied to the steady-state level of the financial uncertainty. Both panels show improvements over the results in Figure 1 in explaining both price and quantity of financial uncertainties. To illustrate if the marginal contribution is significant, we compute the differences of capital efficiency volatilities estimated with and without the endogenous regime-switching, and Figure 3 compares those with the credit spread and CIU. Results visually confirm that our regime-switching uncertainty model clearly explains data. Despite that CIU, measured by cross-sectional dispersion of credit rating, is outside of the model and not at all utilized in the estimation, our model-based financial uncertainty successfully delineates the quantities of uncertainty over time.

A systematic analysis of time-varying transition calls for proper extension of the model of constant transition. A reasonable assumption is to have regime dynamics of financial conditions tied to economic fundamentals. To this end, we adopt the feedback mechanism of Chang et al. (2017), in which the transition probabilities are functions of historical shocks. The regime-switch is determined by a stationary AR(1) regime factor and a threshold parameter. It is a normal regime if the regime factor is below the threshold, and a distress regime otherwise. The innovation of the regime factor can be decomposed into a linear combination of past fundamental shocks and an exogenous innovation. The vector of coefficients has a unit length by construction. Therefore the squares of the coefficients may be interpreted as percentage contributions of the corresponding shocks to the regime shifts. States of the uncertainty process identify the financial regimes. We estimate the model on 1981Q1-2019Q3 data. As seen from the previous figures, the estimated uncertainty explains drops in corporate bond spreads observed in the mid-1990s and mid-2000s much better compared to the fixed-regime model.[2]

We quantify the contribution of each of the structural shocks to changes in agents' outlook of financial markets. Financial conditions ridden with frictions are time-

[2]We also tried exogenous regime-switching models to compare and find that our endogenous regime-switching model outperforms in this regard. Results are readily available upon request.

varying and affect forming expectations of economic agents, and their decisions, in turn, have feedback effects in determining future capital market conditions. Moreover, this helps to identify uncertainty shocks by teasing out fundamental economic and financial shocks.

Our result states that structural shocks explain a significant portion of the variation in the regime factor, yet independent fluctuations in uncertainty shocks exist and vary over time.[3] Our estimation results state that dynamic responses to the SS-uncertainty shock differ entirely from those to other fundamental shocks, both qualitatively and quantitatively. This shock affects transition probabilities directly. Partly due to the persistence of SS-uncertainty regimes, the direction of this shock often does not matter, and its dynamic effect depends mostly on which regime the economy belongs to at the impact date. Inertia and asymmetric effects prevail as a result. Specifically, in the high (low) SS-uncertainty regime, economic activities decrease (increase) regardless of the shocks' direction. For a large shock or when the economy experiences transitions, this shock has more symmetric effects. Economists are often puzzled by anomalous responses of crucial economic variables against shocks affecting the degrees of risk and uncertainty. Our volatility setup can explain such seemingly counterintuitive results. Overall, we believe that our model identifies an uncertainty shock that has distinctive propagation channels.

The paper proceeds as follows. Section 2 relates this paper to the literature. Section 3 explains the model. Section 4 discusses the effects of switching financial conditions and reports estimation results. Section 5 presents our main results. Then, we conclude. We leave a description of the economic model and its solution, estimation, and filtering procedures in the Appendix, and provide additional details of the numerical procedures we implement in the Online Appendix.

[3]Quantitatively, investment-specific shocks, firms' net worth, investment efficiency, monetary and fiscal policies shocks are important with time-varying degrees. Qualitatively, variables related to decreases in adjustment costs tend to improve the financial conditions, while the variables associated with possibly more financing and resource needs such as net worth shocks tend to deteriorate future financial conditions, creating a more pessimistic future outlook. Related, monetary and fiscal policies are likely to lower the degree of financial uncertainty in bad times, which is consistent with the story of public liquidity provision.

2 Literature

The relation between uncertainty and output growth in the business cycle frequency, and the transmission mechanism from one to the other, has received substantial attention since the influential work of Bloom (2009). Uncertainty is a key suspect of the depth of the Great Recession. Proxies of uncertainty rise sharply with NBER-based recessions and financial markets react ((Bloom, 2009; Kim et al., 2009; Bloom et al., 2018; Jeong et al., 2015; Jurado et al., 2015; Baker et al., 2016; Chang et al., 2016; Kim et al., 2020)). Evidence from a dynamic factor model suggests that two classes of highly correlated shocks, namely, credit supply and financial/political uncertainty, were the primary drivers of variation in growth of detrended GDP and employment during the Great Recession (Stock and Watson, 2012).[4]

Models on the real-option channel typically predict a relatively quick overshooting of output several periods after the initial reduction due to high uncertainty. The slow recovery following the great slump thus presents a challenge as Bachmann et al. (2013) in a VAR analysis with standard recursive identification strategy detect no evidence suggesting quick rebound and overshooting effect in the U.S. data. Gilchrist et al. (2014) provide strong VAR evidence suggesting credit spread as a critical conduit of uncertainty transmission in the U.S. during 1963Q3 - 2012Q3, and theorize that increases in firm risk lead to a rise in bond premia and the cost of capital which, in turn, triggers a prolonged decline in investment activity. Christiano et al. (2014) demonstrate that fluctuations in uncertainty can generate sizable and persistent reductions in output and argue it is the primary determinant of the US business cycle using an estimated medium-scale DSGE model with BGG financial friction, a sharply different result concerning the contribution of a conventional set of structural shocks compared to the estimated model of Christiano et al. (2005). Moreover, Caldara et al.

[4]This paper also relates to works concerning policy effectiveness in an economy with uncertainty. On the one hand, the real-option effect in uncertain times implies temporarily less effective fiscal policies because firms are more cautious in responding to price changes due to irreversible investment (Bloom et al., 2018). On the other hand, in line with real-option theory, evidence from structural VARs suggests dampened effects of monetary policy shocks in more uncertain times (Aastveit et al., 2017). Additionally, the effect of monetary policy instruments on macro variables is at best indirect (Bernanke and Kuttner, 2005). Monetary policy actions more directly influence financial markets by affecting asset prices and returns. Empirically, monetary policy surprises are shown to significantly impact asset prices, which is primarily associated with changes to risk premia (Bernanke and Kuttner, 2005; Drechsler et al., 2018).

(2016) employ a VAR model identified via the penalty function approach and posit that the Great Recession is likely a consequence of the interaction of acutely elevated uncertainty and tightened financial constraint.

Another strand of relevant literature regards the effects of expectation formation. In a DSGE model, Liu et al. (2011) examine the importance of expectation formation effects of regime-switching on monetary policy. They show that the possibility of regime shifts in policy can significantly influence agents' expectation formation and equilibrium dynamics. Bianchi (2013) estimates a DSGE model with switching monetary policy regimes and finds that if agents in the 1970s had anticipated a more aggressive response to inflation by the Federal Reserve, inflation would have been lower. Bianchi and Ilut (2017) extend this work by allowing a mixture of monetary-fiscal policy regimes.

On the topic of uncertainty and time-varying financial friction, this paper is related to Linde et al. (2016). They demonstrate the macroeconomic implications of financial market friction in a medium-scale DSGE model with BGG financial accelerator and regime-switching monitoring cost, without further discussion of the expectation effect. By modeling switching monitoring cost, they generate non-zero predictive density on observing the low output growth in 2008Q4.[5]

There are three essential differences in our approach. First, their results rest heavily upon the specification of the Markov-switching SVAR, and ours do not. Second, they assume a first-order log-linear approximation of the Markov-switching DSGE solution around a regime-independent steady state, whereas we solve the regime-switching DSGE model around two regime-specific steady states. Third, we include feedback channels to regime transition so that we may more coherently discuss the effect of expectation induced by time-varying transition probabilities.[6]

[5]Extending this work, Lhuissier and Tripier (2021) estimate a similar model by minimizing the distance between the impulse responses of an identified Markov-switching SVAR, and those of a medium-scale Markov-switching DSGE. Driven by the Markov-switching SVAR evidence, they conclude that the amplification effect of financial friction diminishes as agents grow more confident in their outlook of the financial market.

[6]On regime-switching with time-varying transition probabilities in DSGE models, Benigno et al. (2020) consider switching between a financially constrained state and a non-binding state, with switching probabilities depending on the indebtedness of agents. On the other hand, we use regimes to define the steady-state level of volatility related to entrepreneurial capital efficiency, which depend on the full set of fundamental shocks.

Table 1: List of Fundamental Shocks and Feedback Parameters

Shocks	Feedback	Label
ϵ_t	$\rho_{v,\epsilon}$	Transitory Technology Shock
$\mu_{z^*,t}$	ρ_{v,μ_z}	Persistent Technology Growth Shock
g_t	$\rho_{v,g}$	Government Spending Shock
$\epsilon_{p,t}$	$\rho_{v,p}$	Monetary Policy Shock
π_t^*	ρ_{v,π^*}	Inflation Target Shock
$\mu_{\Upsilon,t}$	ρ_{v,μ_Υ}	Investment-Specific Shock
γ_t	$\rho_{v,\gamma}$	Equity Shock
$\lambda_{f,t}$	ρ_{v,λ_f}	Price Markup Shock
$\zeta_{c,t}$	ρ_{v,ζ_c}	Preference Shock
$\zeta_{i,t}$	ρ_{v,ζ_i}	Marginal Efficiency of Investment Shock

Notes: This table presents a complete list of fundamental shocks along with their feedback parameters and labels.

3 Model

The model features a regime-switching financial accelerator in a steady-state variable on top of a Smets and Wouters (2007) medium-scale DSGE model. Our model under a fixed regime is a special case of CMR in that the model abstracts from term structure, news shocks, and distortionary taxes. A utility-maximizing representative household accumulates raw capital transformed into effective capital by risk-neutral financial firms, and the production of consumption goods uses the latter form capital. Uncertainty is defined as the standard deviation of the distribution for idiosyncratic efficiency of the effective physical capital. We describe the economic model in sections A.1-A.3 of the Online Appendix.

3.1 Shock Processes

Table 1 presents a complete list of fundamental shocks along with their feedback parameters. The log-deviation to steady state of conventional fundamental shocks, follow generic AR(1) processes of form

$$\log(x_t/x_{ss}) = \rho_x \log(x_{t-1}/x_{ss}) + \sigma_{e,x} e_{x,t}. \tag{3.1}$$

The coefficients $\rho_{\epsilon_p} = 0$ and $\rho_\gamma = 0$ for the monetary policy shocks and the equity shock, respectively. As in CMR, we fix $\rho_{\pi^*} = 0.975$ and $\sigma_{e,\pi^*} = 0.0001$ for the inflation target shock to accommodate the downward trend of inflation in the data. The idiosyncratic uncertainty process (σ_ω) follows an autoregressive process, embedding regime-switching steady-state means in addition to the conventional risk shock:

$$\log(\sigma_{\omega,t}/\sigma_{ss,t}) = \rho_\sigma \log(\sigma_{\omega,t-1}/\sigma_{ss,t-1}) + \sigma_{e,\sigma} e_{\sigma,t}, \tag{3.2}$$

$$\sigma_{ss,t} = s_t \underline{\sigma}_{ss} + (1 - s_t)(2\underline{\sigma}_{ss} - \overline{\sigma}_{ss}), \quad \underline{\sigma}_{ss} < \overline{\sigma}_{ss}, \tag{3.3}$$

with the regime indicator $s_t = 1$, indicating the low steady-state uncertainty (SS-uncertainty) regime, and $s_t = 2$ (the high SS-uncertainty regime), following a Markov chain with a 2×2 transition matrix P_t. We view SS-uncertainty regimes as the states of economy observed by market participants who collect and process information to make economic decisions.

3.2 Regime-Switching and Uncertainty

Equation (3.3) states that the steady-state level of uncertainty $\sigma_{ss,t}$ has binary regimes and the following model describes the switching mechanism:

$$s_t = 1 + 1\{w_t \geq \tau\}, \tag{3.4}$$

where τ is a threshold parameter and its driver is a stationary autoregressive process

$$w_t = \alpha_w w_{t-1} + v_t, \quad v_t \sim \mathbb{N}(0, 1). \tag{3.5}$$

Following Chang et al. (2017), we consider intertemporal correlation between the column vector of all historical structural shocks ε_{t-1} and the regime factor innovation v_t of form

$$\begin{pmatrix} \varepsilon_{t-1} \\ v_t \end{pmatrix} \sim \mathbb{N}\left(0, \begin{pmatrix} I & \rho_{\varepsilon,v} \\ \rho'_{\varepsilon,v} & 1 \end{pmatrix}\right), \quad \rho'_{\varepsilon,v}\rho_{\varepsilon,v} < 1 \tag{3.6}$$

where $\rho_{\varepsilon,v}$ is the column vector of correlation coefficients between each structural shock and the regime factor innovation. See a summary of feedback coefficients in

Table 1. The above feedback model is a convenient approach to introduce flexible time-varying conditional expectations formed by economic agents. This is a key departure of our model from the existing ones employing Markov chains with constant transition probabilities. The transition probabilities of staying in Regime-1 at t, $P_{1|1,t}$, and the probabilities of switching to Regime-1 at t from Regime-2 at $t-1$, $P_{1|2,t}$, characterize the time-varying transition matrix P_t. Easy to show that

$$P_{1|1,t} = \frac{\int_{-\infty}^{\tau\sqrt{1-\alpha_w^2}} \Phi_{\rho_{\varepsilon,v}}\left(\tau - \frac{\alpha_w w}{\sqrt{1-\alpha_w^2}} - \rho'_{\varepsilon,v}\varepsilon_{t-1}\right) d\Phi(w)}{\Phi(\tau\sqrt{1-\alpha_w^2})} \tag{3.7}$$

$$P_{1|2,t} = \frac{\int_{\tau\sqrt{1-\alpha_w^2}}^{\infty} \Phi_{\rho_{\varepsilon,v}}\left(\tau - \frac{\alpha_w w}{\sqrt{1-\alpha_w^2}} - \rho'_{\varepsilon,v}\varepsilon_{t-1}\right) d\Phi(w)}{1-\Phi(\tau\sqrt{1-\alpha_w^2})} \tag{3.8}$$

with $\Phi(\cdot)$ denoting the standard normal distribution function and

$$\Phi_{\rho_{\varepsilon,v}}(w) = \Phi\left(\left(1-\rho'_{\varepsilon,v}\rho_{\varepsilon,v}\right)^{-1/2} w\right).$$

$P_{1|1,t}$ and $P_{1|2,t}$ are time-invariant if $\rho_{\epsilon,v} = 0$, and the regime process (s_t) is Markovian in this case. Therefore, the conventional regime-switching DSGE models with constant transition probabilities are encompassed in our framework as a special case. Indeed, Chang et al. (2017) show that, when feedback is not allowed with $\rho_{\varepsilon,v} = 0$, the pair of parameters (α_w, τ) maps one-to-one to a time-invariant transition matrix P characterized by constant transition probabilities $P_{1|1}$ and $P_{1|2}$. Hence a more realistic and flexible setup prevails in our model without losing parsimony.

We project the regime factor innovation v_t onto the space span by ε_{t-1} and decompose

$$v_t = \rho'_{\varepsilon,v}\varepsilon_{t-1} + \left(1-\rho'_{\varepsilon,v}\rho_{\varepsilon,v}\right)^{1/2}\eta_t \tag{3.9}$$

into a feedback term $\rho'_{\varepsilon,v}\varepsilon_{t-1}$ and an innovation term $\left(1-\rho'_{\varepsilon,v}\rho_{\varepsilon,v}\right)^{1/2}\eta_t$, where ε_{t-1} and η_t are standard normal random variables independent of each other. The unit

variance of v_t has decomposition

$$\text{var}(v_t) = \sum_i \rho_{\varepsilon,v_{(i)}}^2 + (1 - \rho'_{\varepsilon,v}\rho_{\varepsilon,v}) \tag{3.10}$$

in which $\rho_{\varepsilon,v_{(i)}}$ is the i-th element of the vector $\rho_{\varepsilon,v}$. Since the regime factor w_t is driven by its innovation v_t, we may interpret $\rho_{\varepsilon,v_{(i)}}^2 \times 100\%$ as the percentage contribution of the i-th structural shock to regime shifts. Likewise, $\rho'_{\varepsilon,v}\rho_{\varepsilon,v} \times 100\%$ is the total contribution of structural shocks to regime shifts in percentage term. Moreover, there is an MA(∞) representation of w_t by stationarity

$$\begin{aligned} w_t &= \sum_{k=0}^{\infty} \phi_k v_{t-k} \\ &= \sum_{k=0}^{\infty} \phi_k \left(\rho'_{\varepsilon,v}\varepsilon_{t-1-k} + \left(1 - \rho'_{\varepsilon,v}\rho_{\varepsilon,v}\right)^{1/2} \eta_{t-k} \right), \end{aligned} \tag{3.11}$$

with $\phi_k = \alpha_w^k$ for $k = 0, 1, 2, \cdots$. Hence the latent factor w_t is a linear function of the historical structural shocks and the factor innovations to the infinite past. For an intuitive explanation, in the case of $\rho'_{\varepsilon,v}\rho_{\varepsilon,v} \approx 1$, the latent factor w_t can be approximated by a linear function of the historical structural shocks

$$w_t \approx \sum_{k=0}^{\infty} \phi_k \rho'_{\varepsilon,v}\varepsilon_{t-1-k}, \tag{3.12}$$

and can potentially be expressed as a function of historical state variables. Related, the difference between equations (3.11) and (3.12) reveals how the history of the exogenous uncertainty shocks contributes to regime-switching in the steady-state level of uncertainty.

As mentioned earlier, if a volatility variable measures risk and uncertainty, our model in equations (3.3) to (3.9) distinguishes the expectation shock (v_t) from the $e_{\sigma,t}$ shock, because the former shock operates mainly through the expectation channel. If the economy is in one SS-uncertainty regime and likely to stay in the same regime, the effect of v shock mainly depends on the regime that the economy belongs to. Suppose there exists a small v shock that perturbs the probabilities of regime switches. If the probability p of being in the low SS-uncertainty regime is close to 1, a small shock

will result in a similar switching probability regardless of the direction of the shock (e.g., for a small v shock $\epsilon > 0$, both $p - \epsilon$ and $p + \epsilon$ will be close to 1). If an agent makes economic decisions, such as investment, it is likely that she increases (decreases) an investment in the low (high) steady-state uncertainty environment, and regime-switching probability works as a weight in computing the expectations using the above regime-contingent outcomes. For a simple exposition, consider a response of investment of size $\Delta I_{\sigma_{ss}} > 0$. In the low SS-uncertainty regime, the size of the investment response is going to be $\Delta I_{\sigma_{ss}} > 0$, while it is assumed $-\Delta I_{\sigma_{ss}} < 0$ in case of the high SS-uncertainty regime. Suppose that the economy is currently in the low SS-uncertainty regime ($\underline{\sigma}_{ss}$). Then, in response to a v shock that perturbs the distribution, if the size of the shock (ϵ) is sufficiently small and $p \approx 1$, the expected responses are

$$(p \pm \epsilon)\Delta I_{\sigma_{ss}} + (1 - (p \pm \epsilon))(-\Delta I_{\sigma_{ss}}) = 2(p \pm \epsilon)\Delta I_{\sigma_{ss}} - \Delta I_{\sigma_{ss}}.$$

Thus, if $p \approx 1$ and $\epsilon \approx 0$, the expected responses will be $\Delta I_{\sigma_{ss}}$ for both a positive ($+\epsilon$) and a negative $-\epsilon$ shock. Similarly, if the economy is currently in the high SS-uncertainty regime and unlikely to shift toward the low SS-uncertainty regime (i.e., $p \approx 0$), the response to the expectation shock, provided the size of the shock (ϵ) being small, is going to be ($-\Delta I_{\sigma_{ss}}$) whether the shock is positive or negative. In sum, for a small v shock, the dynamic effects of this uncertainty shock depend critically on the regime with which the economy is faced, and the direction of the shock is relatively unimportant. This is because the uncertainty shock in our model only slightly perturbs the regime-switching probability distribution and is not large enough to move the needle for a switch. This differs both qualitatively and quantitatively from other shocks including the risk shock.

Note that we emphasize the 'size' of this expectation shock in explaining the mechanism of the shock propagation. If this shock is sufficiently large, regime-switching probabilities can change significantly, and the resulting impulse response can be quite different from the above cases. To make it more concrete, suppose first that the economy is right in the middle of regime-switching, and the size of v shock is sufficiently large, then a positive v shock makes the probability of high SS-uncertainty regime much higher and closer to 1, whereas a negative v shock leads to the same probability towards 0. Then, the impulse responses to a sufficiently large v shock are going to

be similar to those to other structural shocks. For a positive uncertainty shock of v, investment decreases, and a negative uncertainty shock increases investment over time. Now suppose another plausible situation where the economy is currently in the low SS-uncertainty regime, but there exists a nontrivial chance of switching to the high SS-uncertainty regime, then it is possible to observe a highly asymmetric response against a positive or negative v shock. For a negative v shock, the shock simply states that the economy is going to continue to stay in the low SS-uncertainty regime. Then, an increase in investment will prevail in response to this reduction in uncertainty. However, when there exists a sizable positive uncertainty shock, the probabilities of the economy in the high and low SS-uncertainty regimes now become similar. If these two probabilities are the same at 0.5, the investment responses are going to be zero. That is, due to the increases in transition to the high steady-state risk regime in a near future, highly muted or no responses can be observed.

Our model has a novel shock propagation mechanism that distinguishes from the conventional models. We believe that our model has potentials to explain seemingly puzzling behaviors of economic variables in a coherent way. In the next section, we estimate our model to verify if our theory is valid and data are consistent with the above explanations.

4 Estimation

This section describes the data and report estimation results for two sample periods. The first set spans from 1981 to 2019. For the second set, a sub-period of 1981 to 2010 is used. The latter set corresponds to the sample used in CMR, hence facilitates comparison.

4.1 Data

The data set contains quarterly observations of eleven variables spanning from 1981Q1 to 2019Q3. All of the variables are in real and per capita terms. There are eight standard aggregate variables in our empirical analyses: GDP, consumption, investment, inflation, real wage, relative price of investment goods, labor hours, and effective federal funds rate.

Table 2: Calibrated Parameters

Parameter	Label	Value
β	Discount rate	0.9987
σ_L	Curvature, disutility of labor	1.0000
ψ_L	Disutility weight on labor	0.7705
$\lambda_{w,ss}$	Steady state, markup, labor	1.0500
μ_z	Growth rate of economy	0.4100
Υ	Trend of investment technology	0.4200
δ	Capital depreciation rate	0.0250
α	Capital share	0.4000
$\lambda_{f,ss}$	Steady state, markup, intermediate good	1.2000
γ_{ss}	Steady state, survival rate of entrepreneurs	0.9850
W_e	Transfer to entrepreneurs	0.0050
η_g	Steady state, spending-to-GDP ratio	0.2000
π^*	Steady state, inflation target	2.4300

Notes: This table presents the parameters we fix *a priori*. The parameter values are set following CMR.

GDP is deflated by its implicit price deflator; real household consumption is the sum of household purchases of non-durable goods and services, each deflated by its implicit price deflator; investment is the sum of gross private domestic investment plus household purchases of durable goods, each deflated by its price deflator. The per capita terms are divided by the population over 16. Annual population data obtained from the Organization for Economic Cooperation and Development are linearly interpolated to obtain quarterly frequency observations. The real wage is the hourly compensation of all employees in non-farm business divided by the GDP implicit price deflator. The short-term risk-free interest rate is the three-month average of the daily effective federal funds rate. The level of inflation is measured as the logarithmic first difference of the GDP deflator. The relative price of investment goods is measured as the implicit price deflator for investment goods divided by the implicit price deflator for GDP. The labor hours are in log (per capita) levels, net of the sample mean.

There are also three financial variables: credit to non-financial firms, net worth of entrepreneurs, and credit spread. The credit to non-financial firms is taken from the flow of funds data set constructed by the U.S. Federal Reserve Board. The entrepreneurial net worth is the Dow Jones Wilshire 5000 index. The credit spread

Table 3: Estimation Results: Regime-Switching Model with Feedback

				1981-2019				1981-2010			
	Priors			Posteriors				Posteriors			
Parameters	Type	Q5	Q95	Mode	Mean	90% HPD		Mode	Mean	90% HPD	
ξ_w	B	0.7	0.9	0.89	0.88	0.87	0.90	0.91	0.92	0.91	0.94
b	B	0.5	0.9	0.95	0.94	0.92	0.95	0.92	0.93	0.91	0.94
σ_a	Γ	1.5	3	2.15	2.14	1.77	2.48	1.99	1.91	1.46	2.35
S''	N	5	15	3.71	3.58	3.27	3.88	3.43	3.43	3.07	3.79
ξ_p	B	0.5	0.9	0.72	0.71	0.69	0.73	0.69	0.68	0.65	0.71
α_π	N	1.5	3	3.44	3.45	3.20	3.71	3.33	3.58	3.30	3.88
ρ_p	B	0.5	0.9	0.84	0.83	0.81	0.85	0.84	0.80	0.77	0.82
ι	B	0.3	0.65	0.36	0.39	0.29	0.49	0.33	0.29	0.20	0.38
ι_w	B	0.3	0.65	0.49	0.47	0.37	0.57	0.35	0.33	0.24	0.42
ι_μ	B	0.3	0.65	0.88	0.88	0.84	0.92	0.80	0.79	0.74	0.85
$\alpha_{\Delta,t}$	N	0.1	0.4	0.21	0.23	0.13	0.34	0.17	0.17	0.05	0.28
ρ_{λ_f}	B	0.6	0.9	0.98	0.98	0.97	0.99	0.98	0.98	0.97	0.99
ρ_{μ_Υ}	B	0.6	0.9	0.99	0.99	0.98	1.00	0.94	0.94	0.91	0.96
ρ_g	B	0.6	0.9	0.96	0.96	0.95	0.97	0.96	0.96	0.94	0.97
ρ_{μ_z}	B	0.01	0.4	0.00	0.01	0.00	0.03	0.00	0.03	0.00	0.06
ρ_ϵ	B	0.6	0.9	0.76	0.76	0.73	0.80	0.73	0.69	0.65	0.74
ρ_σ	B	0.6	0.9	0.88	0.88	0.86	0.89	0.90	0.93	0.92	0.95
ρ_{ζ_c}	B	0.6	0.9	0.67	0.82	0.73	0.90	0.86	0.85	0.80	0.90
ρ_{ζ_i}	B	0.6	0.9	0.96	0.96	0.95	0.96	0.95	0.95	0.95	0.96
$\sigma_{e,\sigma}$	Γ^{-1}	0.01	0.09	0.08	0.07	0.06	0.08	0.11	0.11	0.10	0.12
σ_{e,λ_f}	Γ^{-1}	0.0005	0.0015	0.01	0.01	0.01	0.01	0.01	0.01	0.01	0.01
σ_{e,μ_Υ}	Γ^{-1}	0.002	0.006	0.00	0.00	0.00	0.01	0.01	0.01	0.00	0.01
$\sigma_{e,g}$	Γ^{-1}	0.001	0.0033	0.02	0.02	0.02	0.02	0.02	0.02	0.02	0.02
σ_{e,μ_z}	Γ^{-1}	0.003	0.01	0.01	0.01	0.01	0.01	0.01	0.01	0.01	0.01
$\sigma_{e,\gamma}$	Γ^{-1}	0.003	0.01	0.01	0.01	0.01	0.01	0.01	0.02	0.01	0.02
$\sigma_{e,\epsilon}$	Γ^{-1}	0.003	0.01	0.01	0.01	0.00	0.01	0.01	0.01	0.01	0.01
$\sigma_{e,p}$	Γ^{-1}	0.01	1	0.82	0.81	0.74	0.90	0.74	0.81	0.70	0.93
σ_{e,ζ_c}	Γ^{-1}	0.003	0.01	0.08	0.08	0.06	0.09	0.07	0.07	0.06	0.08
σ_{e,ζ_i}	Γ^{-1}	0.003	0.01	0.19	0.19	0.18	0.19	0.19	0.18	0.18	0.19
α_w	B	0.5	0.95	0.96	0.96	0.94	0.98	0.89	0.87	0.81	0.93
τ	N	0	1	0.29	0.30	-0.05	0.60	0.46	0.64	0.32	0.93
$\rho_{v,\epsilon}$	U	-0.9	0.9	0.13	0.13	-0.09	0.36	-0.11	-0.05	-0.27	0.20
$\rho_{v,g}$	U	-0.9	0.9	-0.17	-0.26	-0.42	-0.07	-0.05	-0.27	0.20	0.05
$\rho_{v,\gamma}$	U	-0.9	0.9	0.61	0.51	0.38	0.63	0.06	0.07	-0.10	0.25
ρ_{v,λ_f}	U	-0.9	0.9	0.07	0.07	-0.11	0.25	0.22	0.00	-0.21	0.22
ρ_{v,μ_Υ}	U	-0.9	0.9	-0.32	-0.24	-0.42	-0.07	-0.17	-0.30	-0.49	-0.11
ρ_{v,μ_z}	U	-0.9	0.9	-0.07	-0.04	-0.23	0.15	0.29	-0.11	-0.34	0.12
ρ_{v,π^*}	U	-0.9	0.9	0.00	-0.04	-0.23	0.19	0.07	0.01	-0.21	0.23
$\rho_{v,\sigma}$	U	-0.9	0.9	0.15	0.09	-0.09	0.29	0.13	-0.04	-0.24	0.15
$\rho_{v,p}$	U	-0.9	0.9	-0.20	-0.25	-0.44	-0.08	-0.28	-0.50	-0.67	-0.31
ρ_{v,ζ_c}	U	-0.9	0.9	0.05	-0.04	-0.24	0.15	0.32	-0.14	-0.30	0.03
ρ_{v,ζ_i}	U	-0.9	0.9	-0.64	-0.54	-0.69	-0.40	-0.78	-0.64	-0.76	-0.50
$F(\bar{\omega})_1$	B	0.003	0.03	0.01	0.00	0.00	0.00	0.01	0.01	0.01	0.01
$F(\bar{\omega})_2$	B	0.02	0.07	0.01	0.00	0.00	0.01	0.01	0.01	0.01	0.02
μ	B	0.1	0.3	0.15	0.28	0.23	0.33	0.14	0.12	0.10	0.15

Notes: B:"Beta distribution"; Γ: "Gamma distribution"; N: "Normal distribution"; Γ^{-1}: "Inverse gamma distribution"; U: "Uniform distribution."

is the difference between the interest rate on Baa-rated corporate bonds and the rate of the 10-Year U.S. Treasury bonds in constant maturity. The credit spread and the risk-free rate are measured in level.[7]

Among all variables, the consumption, investment, credit, GDP, net worth, relative price of investments, and real wages are demeaned first-order log-difference.

4.2 Priors and Posteriors

We estimate the quantitative DSGE model using a Random-Walk Metropolis-Hastings (RWMH) sampler. The time-varying transition matrix in a DSGE model complicates the estimation procedure since the filtering problem within the sampler requires a complete history of regimes in general. For a two-regime model, the computation quickly becomes infeasible as the history unfolds because the total number of paths to track is 2^T with the sample size T.

We apply the Chang et al. (2021) regime-switching filter to overcome the issue of exploding regime history. Instead of introducing another set of notations, we use y_t, x_z and z_t to denote observables, state variables and exogenous variables in this section, and use u_t and ε_t to denote measurement errors and state innovations, respectively. The filter assumes a state space model (SSM) of the form

$$y_t = D_{s_t} + Z_{s_t} x_t + F_{s_t} z_t + Q_{s_t} u_t \tag{4.1}$$

$$x_t = C_{s_t} + G_{s_t} x_{t-1} + E_{s_t} z_t + R_{s_t} \varepsilon_t \tag{4.2}$$

with regime dynamics of (s_t) specified by (3.4) and (3.5) allowing feedback of the form (3.6). Equation (4.1) describes the relationship between data and the state variables in the model. Equation (4.2) is the system of policy functions. The SSM is completed by the time-varying transition probabilities characterized by (3.7) and (3.8). The filter performs the predict-update recursion and takes a marginalizing-collapsing approach to approximate the likelihood function $p(Y_{1:T}|\theta)$. For notational convenience, we do not differentiate the exact and the approximate likelihood, acknowledging that the likelihood is always approximated in our empirical analysis.

[7] Our data set is a subset of CMR. We exclude the term-spread because the term structure is not explicitly modeled in our setup. Additionally, CMR find the term structure to be quantitatively unimportant in their exercises.

Readers are referred to Chang et al. (2021) for a complete description of the filtering algorithm (endogenous-switching Kalman filter), and to Appendix C.1 for a detailed description of the procedure we use.

We partition the parameters into two sets. The first set contains the parameters we set *a priori*. We follow CMR closely in fixing this subset of structural parameters. These parameters are reported in Table 2.[8] Table 3 reports the full sample posterior estimates of our model. We call a feedback channel positive when a positive structural shock further increases the probability of switching to the high-uncertainty regime. Analogously, we call a feedback channel negative when a positive structural shock decreases the probability of switching to the high-uncertainty regime. The only significant positive feedback channel in the model pertains to the net worth shock. The significant negative feedback channels include the investment-specific technology shock, MEI shock, fiscal policy shock, and the monetary policy shock. We observe that most of the posterior mean estimates of the regime-switching and feedback parameters are similar across the full sample (1981-2019) and the CMR sample (1981-2010), and our quantitative results barely change as we use either group of the parameter estimates.

4.3 Sources of Time-varying Transitions and Expectations

An agent with knowledge of w_{t-1} can form the expectation concerning regime s_t easily by comparing its value against threshold τ. It is more likely to have a regime switched if w_{t-1} is close to the threshold. Neither agents in our model nor econometricians observe the regime factor. Nonetheless, its conditional mean can be estimated and serves as a decent proxy for the degree of optimism in agents' expectations from an econometrician's viewpoint.

We obtain the smoothed regime factor at the posterior mean and decompose it using the estimated shocks recursively with the following equation

$$\mathbb{E}(w_t|\mathcal{F}_T) = \alpha\mathbb{E}(w_{t-1}|\mathcal{F}_T) + \rho'\mathbb{E}(\varepsilon_{t-1}|\mathcal{F}_T) + (1-\rho'\rho)^{1/2}\,\mathbb{E}(\eta_t|\mathcal{F}_T). \tag{4.3}$$

Figure 4 reports the conditional mean of the regime factor with the threshold esti-

[8] We set all tax rates at zero because our model does not include the tax on consumption, capital income, and labor income.

Figure 4: Estimated Regime Factor and Threshold

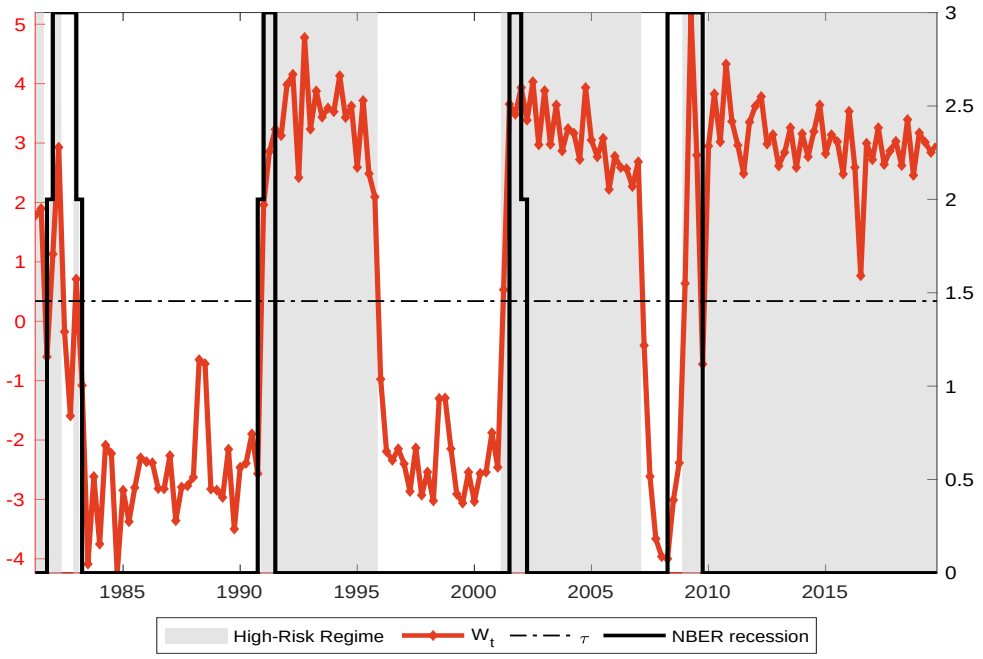

Notes: This figure presents the estimated regime factor w_t, and its implied high-risk regime, and compare them to the NBER recession index. The diamond red curve (left scale) plots the smoothed regime factor w_t computed at the posterior mean of the 1981-2019 sample. The dash-dotted dark line plots the posterior mean of the regime threshold τ. The shaded areas highlight the high-risk regimes identified by times at which $w_t > \tau$. And the solid black line (right scale) reports the NBER recession indicator from the period following the peak through the trough aggregated from monthly frequency to quarterly frequency.

mated at the posterior mean. The high SS-uncertainty regime corresponds to the region above the threshold. Agents, from an econometrician's perspective, become more optimistic (pessimistic) as the regime factor falls deeper in the low (high) SS-uncertainty regime. The estimated regime factor depicts that uncertainty perception dramatically increases during the recession period then stays in the high uncertainty region persistently. Thus, the empirical result suggests that the resolution of uncertainty is slow. The degree of pessimistic outlook on financial condition in the early 1980s recession is weaker by our estimate compared to all later recessions, but it is clear that our estimated high SS-uncertainty regimes are compatible with the U.S. recession periods. Given the size of output contraction, we expect a deeper contraction in consumption and labor hours with slower recovery in a high SS-uncertainty regime,

as demonstrated in the preceding section. Indeed, the "jobless recovery" is a common pattern shared by all major recessions after 1982. The 2008 global financial crisis is also well known for its slow recoveries in investment, output, and consumption.

Figure 5: Historical Decomposition of Regime Factor

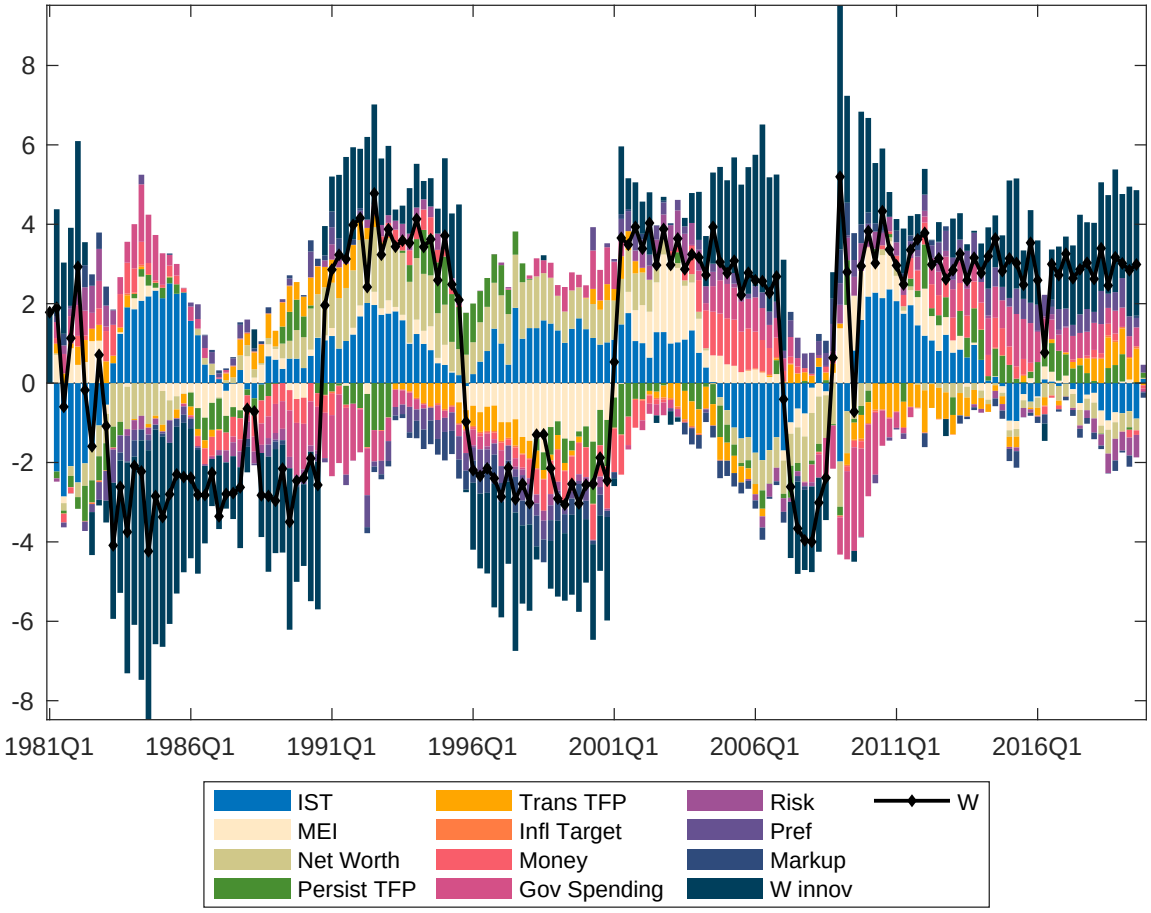

Notes: This figure presents the historical decomposition of the latent regime factor reported in Figure 4 with respect to the smoothed historical shocks computed at the posterior mean of the 1981-2019 sample. The decomposition is produced recursively using (4.3).

The latent regime factor w_t can be written as a linear combination of its lag value, previous structural shocks and an exogenous innovation as shown in (3.11). Figure 5 presents the historical decomposition of the latent regime factor with respect to historical shocks estimated at the posterior mean. At each t, the bars in the stacked bar chart represent the cumulative contributions of the corresponding shocks.

The latent regime factor is persistent, with the posterior mean of its autoregressive coefficient, α_w, at 0.96. This observation translates to the fact that the lag of itself explains a substantial portion of the regime factor dynamics.

Figure 6: Estimated Regime Factor Shock (η)

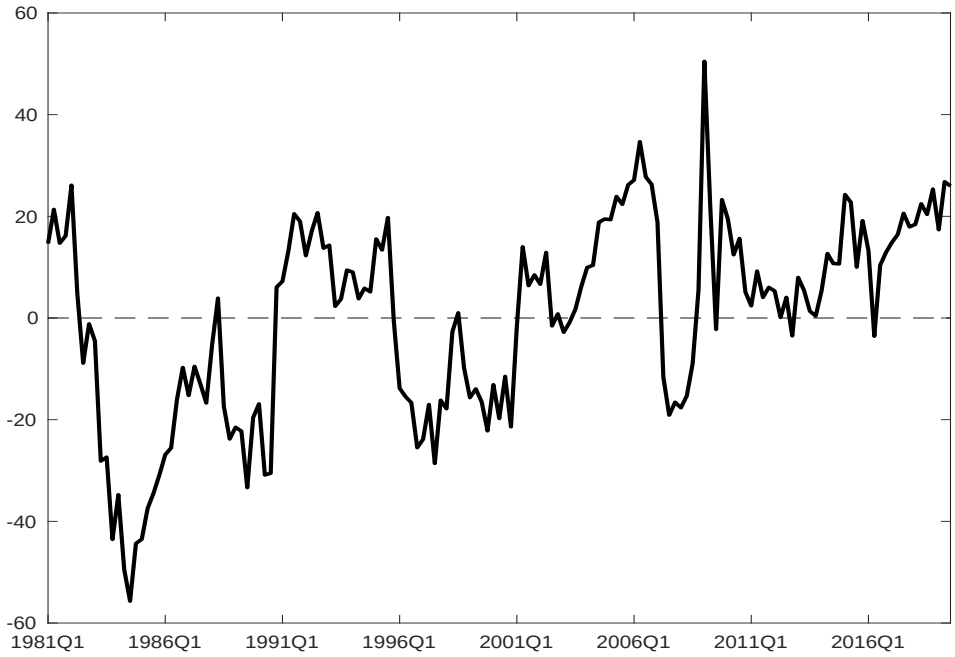

Notes: This figure presents the estimated regime factor shock η computed from (3.11) using smoothed regime factor w and the smoothed structural shocks at the full sample posterior mean.

However, the regime factor innovation η_t also accounts for a rather significant portion of the regime factor. The implied shock size can be as large as about 60 standard deviations by the fact that $\rho'\rho \approx 1$. We regard this SS-uncertainty shock as a key source of uncertainty in financial market condition, distinct from the conventional risk shock. Figure 6 plots the estimated sample path of this new uncertainty shock.[9] The investment-specific shock (IST), the marginal efficiency of investment shock (MEI), and the net worth shock (Net Worth) all account for significant portions of the regime factor throughout the entire sample span. For the most part, the IST shock is quantitatively more important than the MEI shock, but it also works together with the

[9]We also conducted a full set of counterfactual analyses by shutting down one shock at a time, and obtained results that are consistent with those reported in Figure 5. These counterfactual regime factors are available upon request.

MEI shock when pushing the regime factor upward. This observation is evident in the early 1990s, early 2000s, and also in the aftermath of Great Recession. These two shocks also work in opposite directions in the late 1990s and at the onset of the Great Recession. Finally, the net worth shocks by our estimate primarily contribute to the lowering of the regime factor in the 1980s and 2000s.

Figure 7: Estimated Regime Factor and Probability of High Steady-State Uncertainty Regime

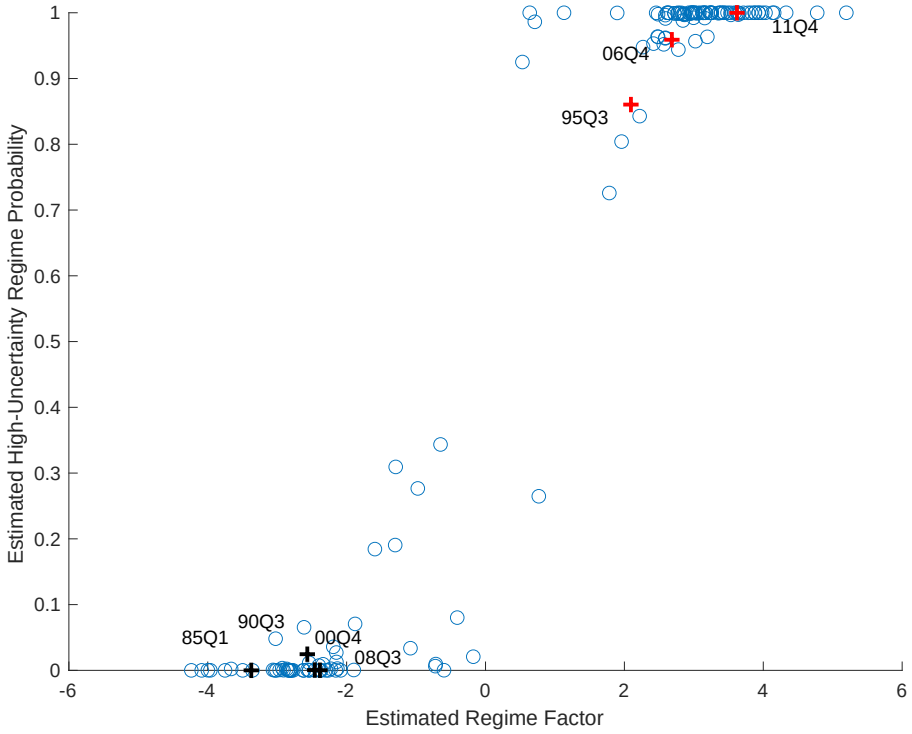

Notes: This figure presents the scatter plot of the latent regime factor in Figure 4 and the corresponding high-uncertainty regime probabilities. The red (black) crosses label selected dates of high (low) high-uncertainty regime probabilities at which we produce regime-dependent impulse responses to uncertainty shocks in Figure 11.

Both transitory and persistent technological growth shocks are quantitatively important. The persistent TFP shock mainly contributes to the lowering of the regime factor in the early 1990s and early 2000s, and to the rising of the regime factor in the mid-1990s and after the Great Recession. On the other hand, the transitory TFP shock often work in the opposite direction of the persistent TFP shock. It elevates the

regime factor in early 1990s, and lower the factor in mid 1990s and in the aftermath of the Great Recession.

The historical decomposition reveals a substantive role of government in anchoring agents' expectations of the financial market condition. The government spending shock contributes to the lowering of the regime factor substantially in the Great Recession, and the monetary policy shock lowers the regime factor significantly in both of the early-1990s and early-2000s recessions. We argue that this result is natural because the government spending shock and the monetary policy shock reflect the authorities discretion in crisis times. Monetary policy's small effect, relative to the fiscal policy, during the Great Recession is well expected as the federal funds rate reaches the zero lower bound.

According to our model, the probability of an SS-uncertainty regime, the size of expectation shock that moves the regime factor w and the current state of the economy determine the dynamic effects of the uncertainty channel. To better understand the mechanism and how it operates quantitatively, we compute the probabilities of the high SS-uncertainty regime and the regime factor for each time period. Figure 7 plots them as pairs and it clearly demonstrates how they are related. First, low (high) w values correspond to the low (high) probabilities of the high SS-uncertainty regime. However, it is of critical importance to observe that there exist wide intervals of w values that correspond to either 0 or 1 for the high SS-uncertainty regime probabilities. This confirms our economic story that once an economy enters an SS-uncertainty regime, it is likely to stay in the same regime for a while, unless very large shocks hit the economy. An important implication of this evidence is that the rigidity of perception about SS-uncertainty affects the directions of impulse responses. If the size of the uncertainty shock is sufficiently big, conventional impulse responses will prevail. However, for a small uncertainty shock, the direction of the impulse responses depends on the current SS-uncertainty regime. The next section quantitatively investigates these hypotheses.

5 Quantitative Results

This section studies the effects of uncertainty shocks. We also report results related to other structural shocks to investigate the importance of our expectation-augmenting

feedback channels.

5.1 Impulse Response Functions

We construct conventional impulse response functions (IRFs) for a vector of endogenous variables X_t to structural shocks. The IRFs are defined given initial state X_0, initial regime s_0, and a baseline transition probability matrix P when there is no shock. We denote a size-one change to the j-th structural shock at time t by $e_t^j = (0, \cdots, 0, 1, 0, \cdots, 0)$, and denote zero shocks before and after t by e_{-t}^0. We use e^0 to represent zero shocks for all time. Equipped with these conditions, we ask how a structural shock affects the conditional expectation about future regimes of financial market condition to formally define the h-step ahead impulse response as

$$\text{IR}_x^P(h, e_1^j, s_0) = \mathbb{E}^P(X_h|s_0, X_0, e_1^j, e_{-1}^0) - \mathbb{E}^P(X_h|s_0, X_0, e^0) \tag{5.1}$$

where $\mathbb{E}^P(\cdot)$ is the expectation with respect to the baseline transition probability matrix P which subjects to further perturbation by structural shocks through feedback channels. This impulse response is produced recursively for $h = 1, 2, \cdots$. Let $(T_i, R_i), i = 1, 2$ be the regime specific solutions solved around the corresponding steady states $X_i^{ss}, i = 1, 2$ of X_t.[10] For $h = 1$,

$$\text{IR}_x^P(1, e_1^j, s_0) = \big[R_1 P(s_1 = 1|s_0) + R_2 P(s_1 = 2|s_0)\big] e_1^j$$

in which $P(s_1 = i|s_0), i = 1, 2$ are the baseline transition probabilities given s_0. For $h \geq 2$,

$$\begin{aligned}
\text{IR}_x^P(h, e_1^j, s_0) = &[X_1^{ss} + T_1(\mathbb{E}^P(X_{h-1}|s_0, X_0, e_1^j, e_{-1}^0) - X_1^{ss})]P(s_h = 1|s_0, e_1^j, e_{-1}^0) \\
&+ [X_2^{ss} + T_2(\mathbb{E}^P(X_{h-1}|s_0, X_0, e_1^j, e_{-1}^0) - X_2^{ss})]P(s_h = 2|s_0, e_1^j, e_{-1}^0) \\
&- [X_1^{ss} + T_1(\mathbb{E}^P(X_{h-1}|s_0, X_0, e^0) - X_1^{ss})]P(s_h = 1|s_0, e^0) \\
&- [X_2^{ss} + T_2(\mathbb{E}^P(X_{h-1}|s_0, X_0, e^0) - X_2^{ss})]P(s_h = 2|s_0, e^0)
\end{aligned}$$

Appendix D.1 presents the detailed derivation of the above equations. As demonstrated in preceding discussions, the conditional regime probability $P(s_h|s_0, e_1^j, e^0)$ is

[10] We consider regime specific solutions of form $x'(x, e) = X_i^{ss} + T_i(x - X_i^{ss}) + R_i e$ for $i = 1, 2$.

a function of the shock e_1^j because of the feedback mechanism. Let $P_{1,j}$ be the transition matrix perturbed by shock e_1^j. If $s_0 = 1$, for example, we may use the following conditional regime probabilities

$$\left(P(s_h = 1|s_0 = 1, e_1^j, e_{-1}^0),\ P(s_h = 2|s_0 = 1, e_1^j, e_{-1}^0)\right) = (1,0)\times P\times P_{1,j}\times P^{h-2}. \tag{5.2}$$

to weight the regime-dependent responses in the preceding computation of impulse responses of the endogenous variables to the structural shocks.

To elicit effects of a pure expectation shock associated with our SS-uncertainty process, we construct an impulse response function to a shock only to the expectation, and with all structural shocks fixed at zero. Recall that, for the regime factor

$$w_t = \alpha_w w_{t-1} + v_t, \quad v_t \sim_{i.i.d} \mathbb{N}(0,1)$$

we may decompose the factor innovation

$$v_t = \rho' e_{t-1} + (1-\rho'\rho)^{1/2}\eta_t, \quad \eta_t \sim_{i.i.d} \mathbb{N}(0,1).$$

We consider a one-period perturbation e_1^η of size one to the mean of η_t at $t = 1$.This one-time perturbation results in a one-time change in the transition probability matrix P that governs the regime-change from $t = 0$ to $t = 1$. We denote the perturbed transition matrix by $P_{0,\eta}$. The impulse response function is defined as

$$\mathrm{IR}_x^P(h, e_1^\eta, s_0) = \mathbb{E}^P(X_h|s_0, X_0, e_1^\eta, e^0) - \mathbb{E}^P(X_h|s_0, X_0, e^0) \tag{5.3}$$

and is generated recursively for $h = 1, 2, \cdots$. For $h = 1$,

$$\begin{aligned}\mathrm{IR}_x^P(1, e_1^\eta, s_0) = {} & [X_1^{ss} + T_1(X_0 - X_1^{ss})]\left\{P(s_1 = 1|s_0, e_1^\eta) - P(s_1 = 1|s_0)\right\} \\ & + [X_2^{ss} + T_2(X_0 - X_2^{ss})]\left\{P(s_1 = 2|s_0, e_1^\eta) - P(s_1 = 2|s_0)\right\}\end{aligned}$$

For $h \geq 2$,

$$\begin{aligned}\mathrm{IR}_x^P(h, e_1^\eta, s_0) = &\left[X_1^{ss} + T_1(\mathbb{E}^P(X_{h-1}|s_0, X_0, e_1^\eta, e^0) - X_1^{ss})\right] P(s_h = 1|s_0, e_1^\eta, e^0) \\ &+ \left[X_2^{ss} + T_2(\mathbb{E}^P(X_{h-1}|s_0, X_0, e_1^\eta, e^0) - X_2^{ss})\right] P(s_h = 2|s_0, e_1^\eta, e^0) \\ &- [X_1^{ss} + T_1(\mathbb{E}^P(X_{h-1}|s_0, X_0, e^0) - X_1^{ss})]P(s_h = 1|s_0, e^0) \\ &- [X_2^{ss} + T_2(\mathbb{E}^P(X_{h-1}|s_0, X_0, e^0) - X_2^{ss})]P(s_h = 2|s_0, e^0).\end{aligned}$$

Interested readers are referred to Appendix D.2 for a more detailed calculation. In the case that $s_0 = 1$, we use the following conditional regime probabilities

$$\left(P(s_h = 1|s_0 = 1, e_1^\eta, e^0),\ P(s_h = 2|s_0 = 1, e_1^\eta, e^0)\right) = (1, 0) \times P_{0,\eta} \times P^{h-1} \tag{5.4}$$

to weight the regime-dependent responses in the preceding computation of impulse responses of the endogenous variables to the expectation shock.

Our impulse response naturally extends to admit a sequence of shocks $\{e_t^j\}_{t=1,2,\cdots,k}$, as well as a sequence of predetermined regimes $\{s_t\}_{t=1,2,\cdots,l}$ for analysis of the time-varying expectation effect induced by the time-varying transition probabilities. We can further extend this definition to allow for time-varying impulse responses by weighting the state-dependent impulse responses $\mathrm{IR}_x^P(h, e_1^j, s_0)$ with estimated regime probability $P(s_0|\mathcal{F}_0)$ given information $\mathcal{F}_0$ available before the materialization of structural shocks. As a special case, we can compute IRFs by applying unconditional initial regime probabilities as weights.

5.2 Dynamic Responses to Structural and Uncertainty Shocks

We now examine the dynamic responses of consumption, investment, labor hours, and GDP with respect to both structural shocks and the novel uncertainty shock.[11] We begin with the impulse responses given unconditional initial regime probabilities with respect to the shock η, and Figure 8 displays the results. Panels (a) and (b) show the same responses, except that panel (a) also plots the highest posterior density (HPD) regions as credible intervals in conjunction with the impulse responses. In each panel, the first row plots the impulse responses of the macro variables to a positive η shock,

[11] Impulse responses of all other variables are omitted for conserving space and available upon request.

or an increase in the likelihood of the high SS-uncertainty regime. The second row shows the impulse responses when the direction of the η shock is negative, implying that the probability of the low SS-uncertainty regime increases. As explained in Section 3.2, the η shock perturbs transition probabilities across uncertainty regimes, and its responses can vary significantly, depending upon the current regime and the persistence of staying in the same regime. Indeed, the estimated IRFs in Figure 8 shows striking results.

Panel (a) states the following: When uncertainty blows to increase the chance of the high steady-state uncertainty (i.e., a positive shock to η), all the key macroeconomic variables rarely respond. However, when η decreases, to the contrary, investment, hours of work, and output increase. In case of consumption, it initially decreases, presumably due to substitution for investment, then starts increasing after about five periods. These 'highly asymmetric' responses to positive and negative η shocks lead us to examine if the extreme inertial reactions in case of an increase in uncertainty have at least the opposite direction of movement, qualitatively speaking, compared to those cases with a negative η shock. However, the figures in Panel (b) that simply magnify the vertical axes of Panel (a) reveal that both positive and negative η shocks have the same direction: macroeconomic activities increase, regardless of the direction of the uncertainty shock. The only difference is that an increase in uncertainty to the high steady-state regime barely affects real activities, but lower uncertainty shocks significantly increase investment, hours of work, and output.

According to our exposition regarding the novel uncertainty shock and its propagation mechanism in Section 3.2, the observed pattern can arise if the economy is currently in the low SS-uncertainty regime (i.e., when $w_t < \tau$), yet the distance between w_t and τ is relatively short. When there exists a shock that decreases w_t, this makes the switching probability to the high SS-uncertainty regime even lower. Thus, the impulse responses with respect to this distributional shock (η) will be dictated by the low uncertainty regime probabilities. At the same time, an exogenous perturbation that increases the likelihood of migrating to the high SS-uncertainty regime also becomes nontrivial because of the shorter distance of $(\tau - w_t)$. Impulse responses then depend on both regimes that have the opposite signs of reactions. The conditional expectations of future economic performances, defined in equations (5.3) and (5.4), can be close to zero, depending on the degree of transitions from the low to the high

uncertainty regimes.

This is a plausible interpretation consistent with our model. If it is the right interpretation, we should first observe that impulse responses to other structural shocks are much less asymmetric, if not entirely symmetric, due to the feedback channels. Second, if the size of this uncertainty shock is sufficiently large, we can infer that the asymmetry should disappear, because a large deviation from the existing transition probability implies a much higher likelihood of switching regimes to the respective direction of the shock. Thus, in this case, we expect usual, symmetric impulse responses. Third, if we face different distances between the current w and the threshold τ, one should observe highly regime-dependent and counter-intuitive responses. That is, if w is far above τ or the economy is in the high SS-uncertainty regime, regardless of the direction of η shock, impulse responses will look like those to a bad risk shock. If, to the contrary, w is well below τ, impulse responses resemble those to a good risk shock, whether the uncertainty shock is positive or negative.

We test the above three hypotheses. Figures 9-11 plot the appropriate impulse response functions to verify each conjecture. Figure 9 plots the impulse responses of the key macro variables with respect to eight structural shocks but not our new uncertainty shock η. They show highly symmetric responses, at least qualitatively. Thus, it is correct that our novel uncertainty shock differs from other shocks, and our computation procedure is well executed. Second, we check if a large uncertainty shock resolves the issues presented in Panel (a) of Figure 8. Figure 10 plots the impulse responses to five standard deviation η shocks. Now the impulse responses look much more conventional, though some level of quantitative asymmetry exists, due to the current location of w and the estimated value of τ. Thus, when the magnitude of the shock is large enough to lead to a shift in the average perception of financial risk and uncertainty, the propagation mechanism operates like a conventional shock. However, this case is rare. For the most part, shocks are of small magnitudes, and economic responses to the shocks affecting probability assessment can depend on the regime, the speed of transition may be slow, and the resultant reactions can be inertial or very regime-specific. The results suggest that our model may be able to explain various puzzling economic and financial market behaviors when there exist shocks associated with risk and uncertainty of an economy.

As the third conjecture stated, we check if the impulse responses with respect to

the uncertainty shock η differ across the regimes of steady-state uncertainty. Figure 4 shows that several episodes of the high and low steady-state uncertainty regimes exist, and we can use those to draw the impulse responses to the uncertainty shock hitting the economy in the low or high regimes of uncertainty. Based on our estimated regimes, the three periods, 1995Q3, 2006Q4, and 2011Q4, belong to the high steady-state uncertainty regime, and the following four periods, 1985Q1, 1990Q3, 2000Q4, and 2008Q3, are from the low steady-state risk regime. Figure 11 presents the corresponding IRFs for the low (high) uncertainty periods plotted in black (red). As we conjectured, the results are highly regime-dependent, and the direction of the shock does not matter at all. In a low uncertainty period, where the average perception of financial risk and uncertainty is low, perturbations in probability distribution increase economic activities over time. We observe the exact opposite in the case of a high uncertainty period. Any news on uncertainty is bad news. Does this pattern vary quantitatively, depending on the period? We expect the regime dependence results to prevail more or less, depending on the location of the economy in terms of the regime factor and threshold. Figure 11 shows the pattern, especially in the high uncertainty regime (i.e., red-colored responses), consistent with our arguments above, in that impulse responses with different initial regimes show quantitative differences. In conjunction with Figure 4, the initial regimes proximate to a transition lead to fewer fluctuations than otherwise. Nevertheless, the regime dependence of impulse responses irrespective of the direction of the uncertainty shock is largely intact and significant.

Finally, our model allows structural shocks in the previous period to affect transition probabilities of regimes in steady-state risks, and therefore it is worthwhile to check if this feedback channel has quantitative impacts on the impulse responses against other structural shocks. From (4.3) and Figure 5, it is clear that past shocks ε_{t-1} feed into the expectation equation for the regime factor w_t and the unexplained part involving the uncertainty shock η_t constitutes a significant portion of the regime factor. Figure 12 reports the impulse responses weighted by unconditional initial regime probabilities to the same set of eight structural shocks with and without the feedback channels. The dashed lines display the counterfactual impulse responses obtained by turning off the feedback channels, while the solid lines present those from our benchmark model with the feedback channels open. The historical decom-

position of the regime factor in Figure 5 suggested that several shocks such as the MEI shock, the IST shock, and in particular, the net worth (equity) shock significantly contribute to the fluctuations of the regime factor w. The IRF results indeed show that these feedback channels operate significantly for the case of these shocks related closely to firm decisions. In case of a shock to the marginal efficiency of investment, or an investment adjustment cost shock ($\zeta_{i,t}$), the feedback channel strengthens the effect of the MEI shock. Regarding the net worth shock, an increase in equity has more muted dynamic responses with an active feedback channel than otherwise. Perhaps, unexpected, positive shocks in equity value may increase concerns about future economy, leading to the more cautious responses. In case of policy-related shocks, impulse responses with feedback have relatively small deviations from those without feedback. However, Figure 5 shows that monetary policy and government spending shocks sometimes contribute significantly to the fluctuation of the regime factor. Thus, we suspect that policy shocks can have conditional effects in forming expectations. Taken together, while individual contributions are somewhat limited, as a whole, all the structural shocks account for about 80% of the regime factor fluctuations. This reflects the complexity of an expectation formation process, and at the same time, the importance of the exogenous uncertainty shocks to understand business cycles.

5.3 Discussion

This paper has come a long way to show that our SS-uncertainty switching model can identify new shocks, after teasing out the roles of key economic variables that contribute to the expectation and volatility of those variables. The estimated σ process contains both conventional risks and SS-uncertainty terms. Hence, this is our noisy measure of uncertainty in that both risk and uncertainty affect the evolution of the σ process. We compare the estimated sample path with some of the existing uncertainty measures. Specifically, we use financial uncertainty indices by Jurado et al. (2015) (JLN) and economic policy uncertainty by Baker et al. (2016) (EPU). Panels (a) and (b) of Figure 13 display the result. All the measures show that there is a common trend, and our measure is successfully picking the US recession periods recorded by the NBER. Interestingly, adjusting for scales, our measure is

higher when compared to the JLN and EPU measures during the 1990 to 1998 and post-2010 periods. Note that there was a Peso crisis, Asian crisis, Russian debt crisis, and Brazilian Devaluation in the 1990s, and after the 2007-2008 financial crisis, various European sovereign debt crises, followed by the COVID-19 shock in 2020. It appears that our measure does a decent work in capturing the era of uncertainty. One conundrum that applies to all three measures would be that the level of the indices are quite low in 2006-2008. Several draconian economic events have been unraveling during this period, and the period should be filled with uncertainty. Panels (c) and (d) of Figure 13 confirm this conjecture. Uncertainty shocks (η) that move the regime factor w increased substantially over this period. In addition, the estimated uncertainty shocks feature several distinctive patterns that are in line with the various adverse economic and financial events in which uncertainty was rising.

6 Conclusion

In economic and financial decision-making, economic agents may heuristically view that the average perception on future states of risk and uncertainty is either low or high, possibly because of limited information processing ability or other informational frictions. The associated switching probability distribution stochastically evolves, and some exogenous shocks about this probability distribution can arise. Our model and estimation results show that the expectation effect of switching levels of uncertainty exerts a significant impact on the macro-economy, and its channel differs from the conventional risk channels. Our novel uncertainty shock and its propagation mechanism show stark differences in dynamic responses, and the results are sensitive to where the economy is in terms of the mean perception of risk and uncertainty. The proposed model can explain both inertial and abrupt swings of economic variables when there exists a shock increasing or decreasing economic uncertainty in a unified framework. The estimation results related to the uncertainty regime shock suggest that the average level of uncertainty stays long in one regime, once the economy enters it. In particular, we find that the average uncertainty perception sharply increases to the pessimistic regime during recessions, and the heightened level of uncertainty tends to unravel very slowly.

Figure 8: Responses to Uncertainty Shocks

(a) Impulse Responses with HPD Regions

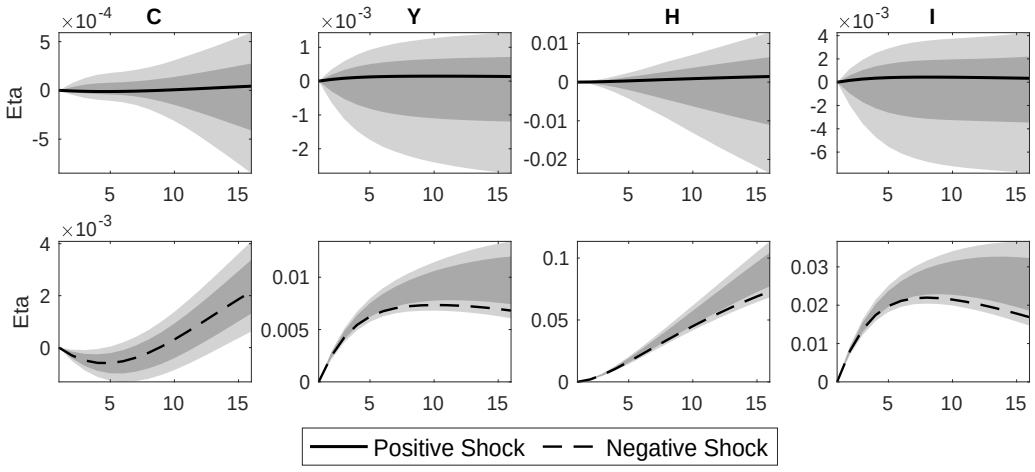

(b) Impulse Responses Only

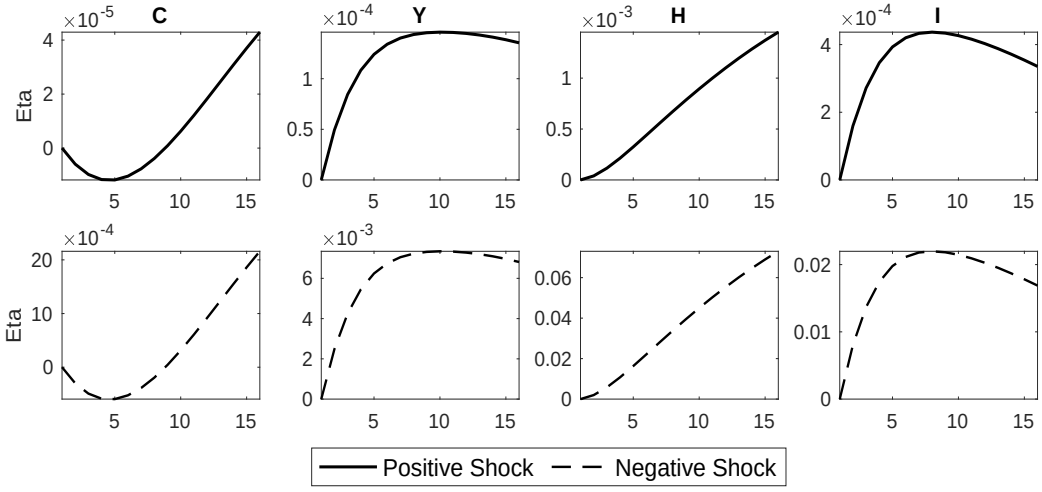

Notes: The figure reports the impulse responses of consumption (C), output (Y), labor hours (H) and investment (I) to positive one-standard deviation uncertainty shocks (η) under unconditional initial regime probabilities. Panels (a) and (b) display the same graphs, except for the vertical scales, because panel (a) plots the highest posterior density (HPD) regions as well. Darker and lighter shaded areas signify 68% and 95% HPD regions, respectively. That is, Panel (b) delineates only the estimated impulse responses. In each panel, the first row (solid line) shows the responses to a positive η shock, whereas the second row (dashed line) plots the response in case of a negative η shock.

Figure 9: Responses to Structural Shocks

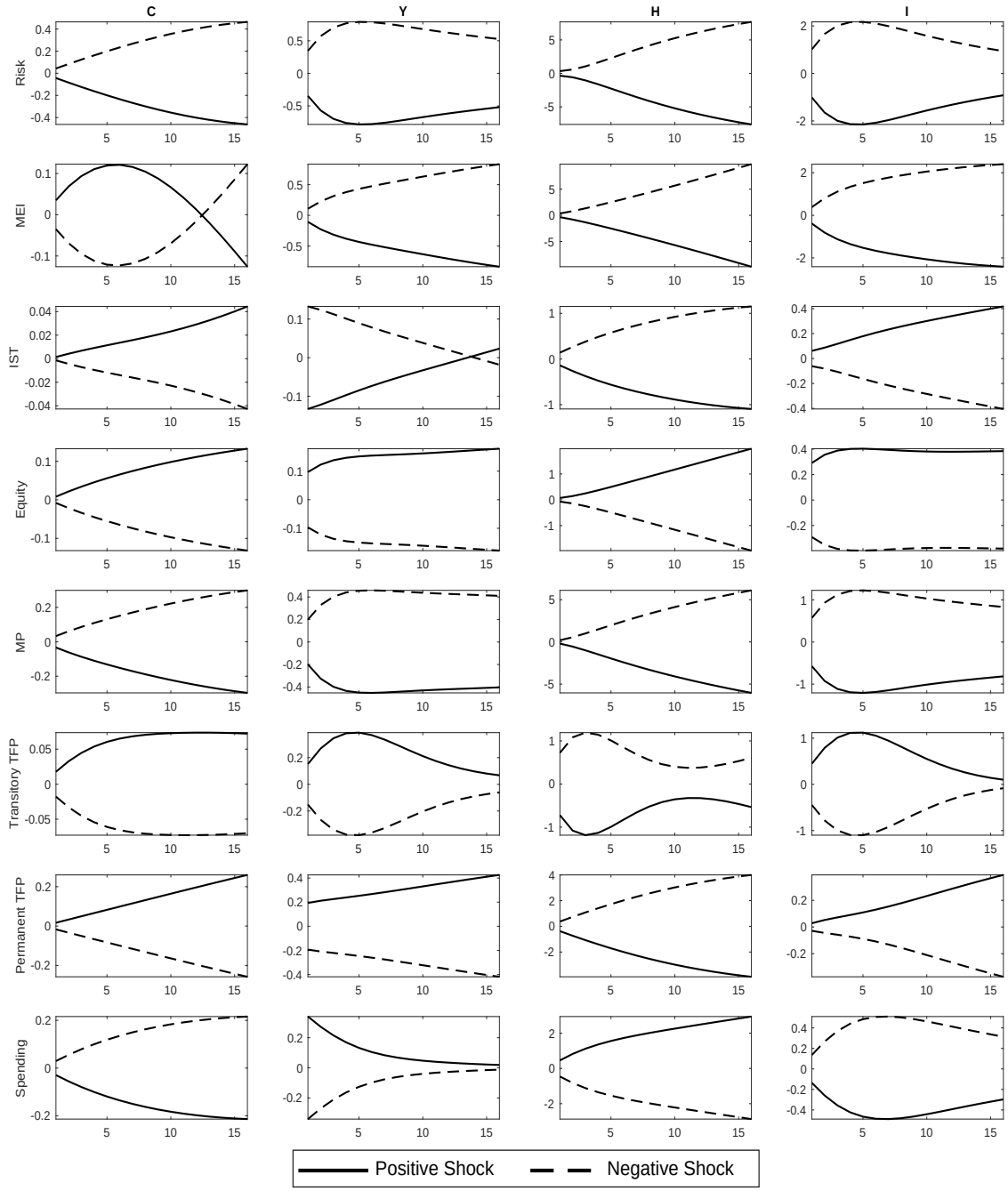

Notes: The figure reports the impulse responses of consumption (C), output (Y), labor hours (H) and investment (I) to positive and negative structural shocks of size one-standard deviation under unconditional initial regime probabilities.

Figure 10: Responses to Large Uncertainty Shocks

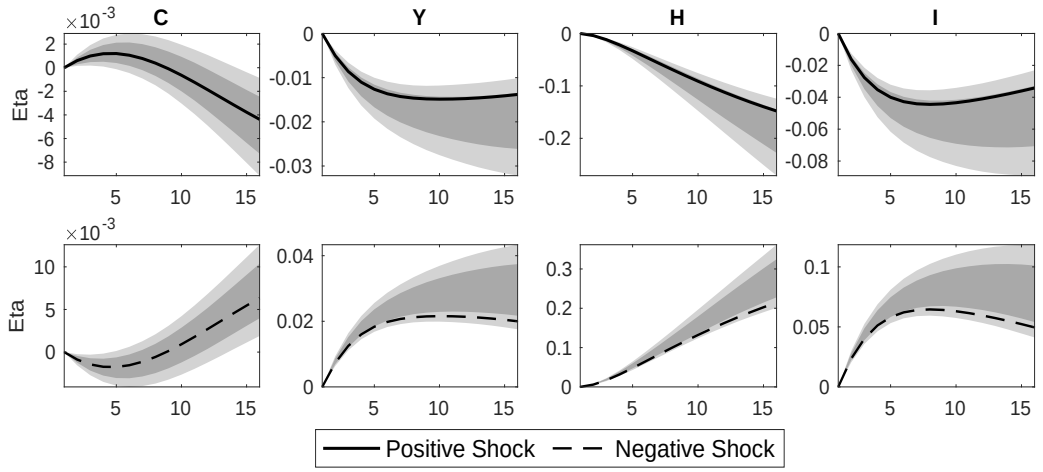

Notes: The figure reports the impulse responses of consumption (C), output (Y), labor hours (H) and investment (I) to large uncertainty shocks of size five-standard deviations under unconditional initial regime probabilities. Darker and lighter shaded areas in each figure signify 68% and 95% highest posterior density (HPD) regions, respectively.

Figure 11: Regime-Dependent Responses to Uncertainty Shocks

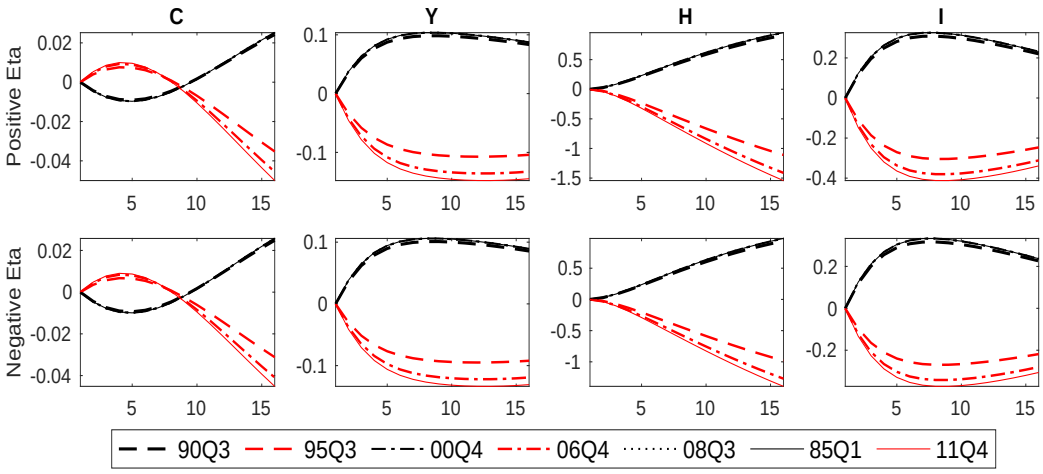

Notes: The figure reports the impulse responses of consumption (C), output (Y), labor hours (H) and investment (I) to positive one-standard deviation uncertainty shocks given initial regime probabilities conditional on information at different times. The red (black) curves label the dates of large (small) high-risk regime probabilities at which we produce regime-dependent impulse responses.

Figure 12: Impulse Responses to Structural Shocks with and without Feedback

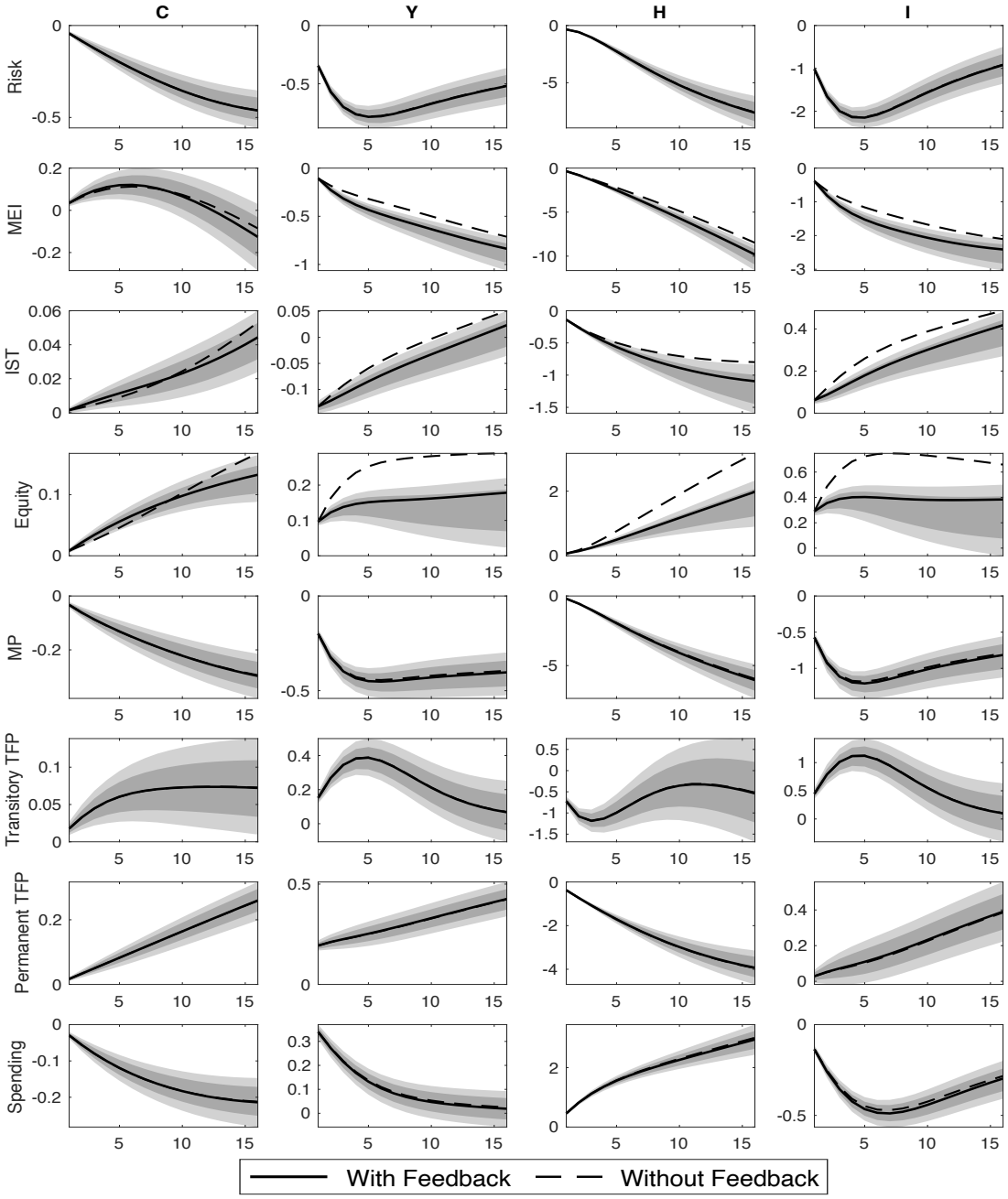

Notes: The figure reports impulse responses of consumption (C), output (Y), labor hours (H) and investment (I) to positive one-standard-deviation structural shocks with and without feedback under unconditional initial regime probabilities. The darker (lighter) shaded area in each figure signifies 68% (95%) highest posterior density (HPD) interval.

Figure 13: Risk and Uncertainty: A Comparison

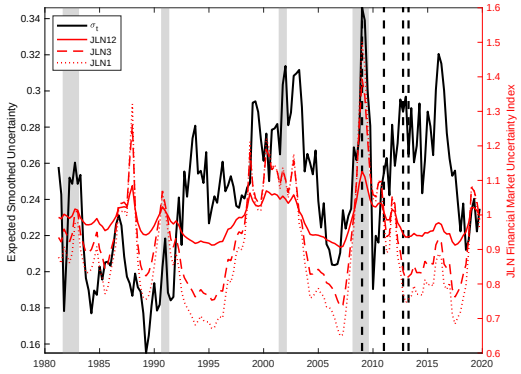

(a) σ vs. JLN

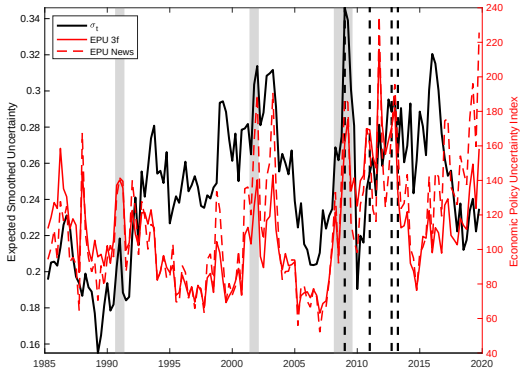

(b) σ vs. EPU

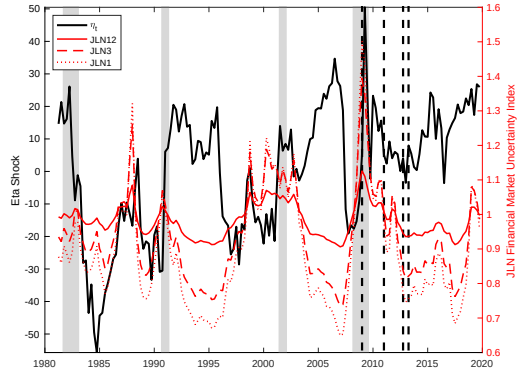

(c) η vs. JLN

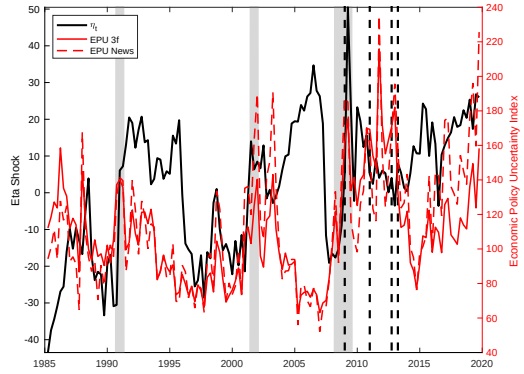

(d) η vs. EPU

Notes: The figure displays the estimated sample paths of the estimated σ (estimated smoothed risk and uncertainty) and the uncertainty shock η_t in comparison with the financial market uncertainty (JLN) indices by Jurado et al. (2015) and the Economic Policy Uncertainty (EPU) indices by Baker et al. (2016). The JLN and EPU indices are the mean values for each quarter computed from monthly frequency data. The shaded areas are NBER recessions, and the dashed vertical lines mark the starting dates of Quantitative Easing (QE1-QE4).

References

Aastveit, K. A., G. J. Natvik, and S. Sola (2017). Economic Uncertainty and the Influence of Monetary Policy. *Journal of International Money and Finance 76*, 50 – 67.

Bachmann, R., S. Elstner, and E. R. Sims (2013, April). Uncertainty and Economic Activity: Evidence from Business Survey Data. *American Economic Journal: Macroeconomics 5*(2), 217–49.

Baker, S. R., N. Bloom, and S. J. Davis (2016). Measuring Economic Policy Uncertainty. *The Quarterly Journal of Economics 131*(4), 1593–1636.

Benigno, G., A. Foerster, C. Otrok, and A. Rebucci (2020, April). Estimating macroeconomic models of financial crises: An endogenous regime-switching approach. Working Paper 26935, National Bureau of Economic Research.

Bernanke, B. S. and K. N. Kuttner (2005). What Explains the Stock Market's Reaction to Federal Reserve Policy? *The Journal of Finance 60*(3), 1221–1257.

Bianchi, F. (2013). Regime Switches, Agents' Beliefs, and Post-World War II U.S. Macroeconomic Dynamics. *The Review of Economic Studies 80*(2), 463–490.

Bianchi, F. and C. Ilut (2017, October). Monetary/Fiscal Policy Mix and Agent's Beliefs. *Review of Economic Dynamics 26*, 113–139.

Bloom, N. (2009). The Impact of Uncertainty Shocks. *Econometrica 77*(3), 623–685.

Bloom, N., M. Floetotto, N. Jaimovich, I. Saporta-Eksten, and S. J. Terry (2018). Really Uncertain Business Cycles. *Econometrica 86*(3), 1031–1065.

Cagetti, M., L. P. Hansen, T. Sargent, and N. Williams (2002). Robustness and pricing with uncertain growth. *The Review of Financial Studies 15*(2), 363–404.

Caldara, D., C. Fuentes-Albero, S. Gilchrist, and E. Zakrajsek (2016). The Macroeconomic Impact of Financial and Uncertainty Shocks. *European Economic Review 88*, 185 – 207. SI: The Post-Crisis Slump.

Chang, Y., Y. Choi, H. Kim, and J. Y. Park (2016). Evaluating Factor Pricing Models Using High-Frequency Panels. *Quantitative Economics 7*(3), 889–933.

Chang, Y., Y. Choi, and J. Y. Park (2017). A New Approach to Model Regimes Switching. *Journal of Econometrics 196*(1), 127 – 143.

Chang, Y., J. Maih, and F. Tan (2021). Origins of Monetary Policy Shifts: A New Approach to Regime Switching in DSGE Models. *Journal of Economic Dynamics and Control*. Forthcoming.

Christiano, L. J., M. Eichenbaum, and C. L. Evans (2005). Nominal Rigidities and the Dynamic Effects of a Shock to Monetary Policy. *Journal of Political Economy 113*(1), 1–45.

Christiano, L. J., R. Motto, and M. Rostagno (2014, January). Risk Shocks. *American Economic Review 104*(1), 27–65.

Drechsler, I., A. Savov, and P. Schnabl (2018). A Model of Monetary Policy and Risk Premia. *The Journal of Finance 73*(1), 317–373.

Gilchrist, S., J. W. Sim, and E. Zakrajsek (2014, April). Uncertainty, Financial Frictions, and Investment Dynamics. Working Paper 20038, National Bureau of Economic Research.

Hansen, L. P. (2007). Beliefs, doubts and learning: Valuing macroeconomic risk. *American Economic Review 97*(2), 1–30.

Jeong, D., H. Kim, and J. Y. Park (2015). Does Ambiguity Matter? Estimating Asset Pricing Models with A Multiple-Priors Recursive Utility. *Journal of Financial Economics 115*(2), 361–382.

Johnson, S. A., H. Kim, and J. H. Kim (2020). Ambiguous Credit Quality and Debt Maturity Structure. In *Western Finance Association 2020 Meetings Paper*.

Jurado, K., S. C. Ludvigson, and S. Ng (2015, March). Measuring Uncertainty. *American Economic Review 105*(3), 1177–1216.

Kim, C.-J. (1994). Dynamic Linear Models with Markov-Switching. *Journal of Econometrics 60*, 1–22.

Kim, H., J. H. Kim, and H. Park (2018). Ambiguity and Corporate Bond Prices. *Available at SSRN 3305605*.

Kim, H., E. Lee, and J. Y. Park (2020). A Consumption-Based Identification of Global Economic Uncertainty. *Available at SSRN 3305605*.

Kim, H., H. I. Lee, J. Y. Park, and H. Yeo (2009). Macroeconomic Uncertainty and Asset Prices: A Stochastic Volatility Model. In *AFA 2010 Atlanta Meetings Paper*.

Kim, H. and J. Y. Park (2018). Risk, Ambiguity, and Stochastic Volatility. *Texa A&M Mays Business School Working Paper*.

Lhuissier, S. and F. Tripier (2021). Regime-Dependent Effects of Uncertainty Shocks: A Structural Interpretation. *Quantitative Economics 12*(4), 1139–1170.

Linde, J., F. Smets, and R. Wouters (2016). Challenges for Macro Models Used at Central Banks. Volume 2 of *Handbook of Macroeconomics*, pp. 2185 – 2262. Elsevier.

Liu, Z., D. F. Waggoner, and T. Zha (2011). Sources of Macroeconomic Fluctuations: A Regime-Switching DSGE Approach. *Quantitative Economics 2*(2), 251–301.

Maih, J. and D. F. Waggoner (2018). Perturbation Methods for DSGE Models with Time-Varying Coefficients and Transition Matrices. Mimeograph, Norges Bank.

Reinhart, C. M. and K. S. Rogoff (2008, May). Is the 2007 US Sub-prime Financial Crisis So Different? An International Historical Comparison. *American Economic Review 98*(2), 339–44.

Smets, F. and R. Wouters (2007, June). Shocks and Frictions in US Business Cycles: A Bayesian DSGE Approach. *American Economic Review 97*(3), 586–606.

Stock, J. H. and M. W. Watson (2012). Disentangling the Channels of the 2007-09 Recession. *Brookings Papers on Economic Activity 43*(1 (Spring)), 81–156.

For Online Publication

Appendix A Economic Model

A.1 The Real Sector

A.1.1 Household

In the model, there is a large number of competitive and identical households. A representative household chooses consumption, investment in physical capital, nominal bond, and differentiated labor $\{C_t, I_t, B_{t+1}, \{h_t(i)\}_{i\in[0,1]}\}$ to maximize the expected discounted utility

$$\max \mathbb{E}_0 \sum_{t=0}^{\infty} \beta^t \zeta_{c,t} \left\{ \log(C_t - bC_{t-1}) - \psi_L \int_0^1 \frac{h_t(i)^{1+\sigma_L}}{1+\sigma_L} di \right\}, \tag{A.1}$$

with $\beta \in (0,1)$ the discount factor, $b \in [0,1)$ the habit formation parameter, σ_L^{-1} the Frisch elasticity of labor hours and ψ_L the labor disutility parameter. In (A.1), $\zeta_{c,t}$ is a preference shock, C_t denotes the per capita consumption, and $h_t(i)$ is the differentiated labor offered by this household. At each period t, the household faces the budget constraint

$$\begin{aligned} P_t C_t + B_{t+1} + \left(\frac{P_t}{\Upsilon^t \mu_{\Upsilon,t}}\right) I_t + Q_{\bar{K},t}(1-\delta)\bar{K}_t \\ = \int_0^1 W_t(i) h_t(i) di + R_t B_t + Q_{\bar{K},t}\bar{K}_{t+1} + \Pi_t, \end{aligned} \tag{A.2}$$

in which P_t is the nominal price for the consumption good, B_t is a one-period nominal bond with rate of return R_t, I_t is the investment good, $\bar{K}_t$ is the physical capital with market price $Q_{\bar{K},t}$, $\bar{K}_{t+1}$ is the end-of-period physical capital, $W_t(i)$ is the wage for the differentiated labor $h_t(i)$, and Π_t is a lump-sum transfer of dividend payment including intermediate goods profits and transfers from entrepreneurs.

Equation (A.2) indicates that the household produces physical capital. After the production of final goods in period t, the representative household produces the

physical capital $\bar{K}_{t+1}$ at the end of the period t, with the technology

$$\bar{K}_{t+1} = (1-\delta)\bar{K}_t + \left(1 - S\left(\zeta_{i,t}\frac{I_t}{I_{t-1}}\right)\right) I_t, \tag{A.3}$$

where $0 < \delta < 1$ denotes the depreciation rate of the physical capital, $S(\cdot)$ is an adjustment cost to investment, and $\zeta_{i,t}$ is the marginal efficiency of investment (MEI) shock. The household has access to a technology that translates one unit of the homogeneous consumption good C_t into $\Upsilon^t \mu_{\Upsilon,t}$ units of investment good I_t with a constant growth rate $\Upsilon > 1$ and an investment technology shock $\mu_{\Upsilon,t}$. The relative price of the investment good in terms of the consumption good is $1/(\Upsilon^t \mu_{\Upsilon,t})$.

The investment adjustment cost function $S(\cdot)$ is an increasing and convex function of form

$$S(\varkappa_t) = \left[e^{\sqrt{S''}(\varkappa_t - \varkappa_{ss})} + e^{-\sqrt{S''}(\varkappa_t - \varkappa_{ss})} - 2\right] \Big/ 2, \tag{A.4}$$

in which $\varkappa_t = \zeta_{i,t} I_t / I_{t-1}$, $\varkappa_{ss}$ is the corresponding steady-state value. The curvature parameter S'' characterizes the cost of (dis)investing away from the steady state.

A.1.2 Goods and Labor Markets

A representative and competitive final good packer combines the intermediate goods $Y_t(j)$ for $j \in [0,1]$ to produce homogeneous good Y_t with the following technology

$$Y_t = \left[\int_0^1 Y_t(j)^{1/\lambda_{f,t}} dj\right]^{\lambda_{f,t}},$$

where $\lambda_{f,t} \geq 1$ is the price markup shock. The j-th intermediate good is produced by a monopolist with the production function

$$Y_t(j) = \max\left\{0, \epsilon_t K_t(j)^{\alpha} (z_t l_t(j))^{1-\alpha} - \Phi z_t^*\right\}. \tag{A.5}$$

The shock to the total factor of production is separated into a stationary technology shock ϵ_t and a shock z_t with a stationary growth rate. In the production function, $K_t(j)$ represents the effective capital which is a constant multiple of the physical capital $\bar{K}_t(j)$. The $l_t(j)$ is the total amount of homogeneous labor employed by the j-

th intermediate good producer. There is a fixed cost Φz_t^* to ensure zero long-run profit in the intermediary good market and to preclude entry and exit at the steady state. As shown in CMR, for the existence of a balanced growth path, $z_t^* = z_t \Upsilon^{(\alpha/(1-\alpha))t}$.

We adopt the Calvo's pricing scheme and allow the j-th intermediate good producer to re-optimize the price $P_t(j)$ with probability $1 - \xi_p$. With probability ξ_p, the producer set the price following $P_t(j) = \tilde{\pi}_t P_{t-1}(j)$ with indexation factor $\tilde{\pi}_t = (\pi_t^*)^{\iota}(\pi_{t-1})^{1-\iota}$. The parameter ξ_p characterizes the price rigidity of the intermediary good market. The inflation rate of the final good Y_t is defined to be $\pi_t = P_t/P_{t-1}$, and π_t^* denotes the inflation target in the monetary policy rule.

A representative and competitive labor contractor demands differentiated labor service $h_t(i)$ for $i \in [0, 1]$ and combines them into homogeneous bundles of labor with the technology

$$l_t = \left[\int_0^1 h_t(i)^{1/\lambda_w} di \right]^{\lambda_w} \tag{A.6}$$

and with wage markup parameter $\lambda_w \geq 1$. The contractor then sells l_t to the intermediate good producers for nominal wage W_t. The differentiated labor suppliers are assumed to adopt Calvo-style frictions. With probability $1-\xi_w$, the i-th differentiated labor supplier optimizes the wage rate $W_t(i)$. If otherwise, the labor supplier follows indexation rule $W_t(i) = (\mu_{z^*,t})^{\iota_\mu}(\mu_{z^*})^{1-\iota_\mu}\tilde{\pi}_{w,t}W_{t-1}(i)$, where μ_{z^*} is the growth rate of z_t^* in the deterministic steady state and $\mu_{z^*,t}$ is the persistent technology shock.[12] In this indexation rule, $\tilde{\pi}_{w,t} = (\pi_t^*)^{\iota_w}(\pi_{t-1})^{1-\iota_w}$. The parameter ξ_w characterizes the wage rigidity in the differentiated labor market.

A.2 Financial Sector

In each of the identical households, there is a large number of risk-neutral entrepreneurs with different levels of initial net worth. After the production in period t, an entrepreneur with net worth $N \geq 0$ borrows $B_{t+1}(N)$ from banks to purchase physical capital $\bar{K}_{t+1}(N)$ from households following

$$Q_{\bar{K},t}\bar{K}_{t+1}(N) = N + B_{t+1}(N). \tag{A.7}$$

[12] Following CMR, the persistent technology growth shock $\mu_{z^*,t} = z_t^*/z_{t-1}^*$.

The physical capital is then turned into efficiency unit $K_{t+1}(N) = \omega \bar{K}_{t+1}(N)$ in production by an idiosyncratic capital efficiency level ω. At each period t, the unit efficiency level ω_{t+1} for each entrepreneur is drawn independently as

$$\omega_{t+1} \sim \text{log-normal}\left(-\frac{\sigma_{\omega,t}^2}{2}, \sigma_{\omega,t}^2\right) \tag{A.8}$$

to ensure a unit mean. In this distribution, $\sigma_{\omega,t}$ is a stochastic process of the level of uncertainty.[13] Upon realization of aggregate rates of return, prices and the efficiency level of the physical capital, the entrepreneur chooses the utilization rate u_{t+1} of the effective capital to maximize the return of capital for a competitive market rate r_{t+1}^k. The gross rate of return in consumption of this entrepreneur is given by $\omega_{t+1} R_{t+1}^k$ with

$$R_{t+1}^k \equiv \frac{(1-\delta)Q_{\bar{K},t+1} + [u_{t+1} r_{t+1}^k - a(u_{t+1})]\Upsilon^{-(t+1)} P_{t+1}}{Q_{\bar{K},t}}. \tag{A.9}$$

This equation means that entrepreneurs receive income by reselling the depreciated physical capital back to households and return of utilized capital after an adjustment cost $a(u_{t+1})$. The adjustment cost $a(\cdot)$ to variable utilization is an increasing and convex function of form

$$a(u) = r^k \left[e^{\sigma_a (u-1)} - 1\right] / \sigma_a. \tag{A.10}$$

The curvature parameter $\sigma_a > 0$ characterizes the cost of capital utilization and r^k is the steady-state rental rate in the model.

At period $t+1$, a portion of the entrepreneurs default when the realized idiosyncratic efficiency shocks to physical capital fall too low. The financial market friction emerges from the asymmetric information between banks and the entrepreneurs because banks do not automatically observe these efficiency shocks to the physical capital. Instead, banks must pay a monitoring cost of proportion μ to the net worth of a borrowing entrepreneur to acquire information of the realized efficiency level.

[13] CMR refer to this process as the risk process associated with entrepreneurial and financing activities, and use the terms risk and idiosyncratic uncertainty interchangeably. Because we extend the volatility to incorporate uncertainty in regimes of steady state values, we refer to this process as uncertainty.

Let $\bar{\omega}_{t+1}$ denote the threshold that separates the repaying entrepreneurs from the defaulting ones. A class of optimal contract dictates that the banks demand a rate of return Z_{t+1} to loans from those repaying entrepreneurs such that

$$\bar{\omega}_{t+1} R^k_{t+1} Q_{\bar{K},t} \bar{K}_{t+1}(N) = B_{t+1}(N) Z_{t+1}. \tag{A.11}$$

For each entrepreneur of net worth N at period t, the law of motion of net worth after receiving transfer W^{ent} follows

$$N_{t+1}(N) = \gamma_t \left[R^k_t Q_{\bar{K},t-1} \bar{K}_t(N) - Z_t (Q_{\bar{K},t-1} \bar{K}_t(N) - N) \right] + W^{ent}, \tag{A.12}$$

where γ_t denotes a net worth (equity) shock. Banks receive zero profit after portfolio diversification in equilibrium. Given price and transfer, the entrepreneur chooses $\bar{\omega}_{t+1}, \bar{K}_{t+1}$ to optimize expected net worth

$$\max \mathbb{E}_t \left\{ [1 - \Gamma_t(\bar{\omega}_{t+1})] R^k_{t+1} Q_{\bar{K},t} \bar{K}_{t+1} \right\} \tag{A.13}$$

subject to the bank's zero-profit condition

$$[\Gamma_t(\bar{\omega}_{t+1}) - \mu G_t(\bar{\omega}_{t+1})] R^k_{t+1} Q_{\bar{K},t} \bar{K}_{t+1} = R_{t+1} B_{t+1}. \tag{A.14}$$

In the preceding equations,

$$\mu G_t(\bar{\omega}_{t+1}) = \mu \Phi(m_t - \sigma_{\omega,t}) \tag{A.15}$$

$$\Gamma_t(\bar{\omega}_{t+1}) = G_t(\bar{\omega}_{t+1}) + \bar{\omega}_{t+1}(1 - \Phi(m_t)) \tag{A.16}$$

denote the expected monitoring cost of banks and the expected gross share of profit going to the banks, respectively, with $\Phi(\cdot)$ being the CDF of a standard normal distribution and

$$m_t = \left(\log \bar{\omega}_{t+1} + \frac{1}{2} \sigma^2_{\omega,t} \right) \Big/ \sigma_{\omega,t}. \tag{A.17}$$

Banks' zero-profit condition implies the leverage ratio

$$\frac{Q_{\bar{K},t}\bar{K}_{t+1}(N)}{N} = \left\{1 - \frac{R^k_{t+1}}{R_{t+1}}\left[\Gamma_t(\bar{\omega}_{t+1}) - \mu G_t(\bar{\omega}_{t+1})\right]\right\}^{-1}. \tag{A.18}$$

The shadow price Λ_t at optimal choice $\bar{\omega}_{t+1}$ is

$$\Lambda_t = \frac{\Gamma'_t(\bar{\omega}_{t+1})}{\Gamma'_t(\bar{\omega}_{t+1}) - \mu G'_t(\bar{\omega}_{t+1})}. \tag{A.19}$$

Clearly, all entrepreneurs choose identical $\bar{\omega}_{t+1}$ such that

$$\mathbb{E}_t\left\{[1 - \Gamma_t(\bar{\omega}_{t+1})]\frac{R^k_{t+1}}{R_{t+1}} + \Lambda_t\left[\frac{R^k_{t+1}}{R_{t+1}}(\Gamma_t(\bar{\omega}_{t+1}) - \mu G_t(\bar{\omega}_{t+1})) - 1\right]\right\} = 0. \tag{A.20}$$

Therefore, the law of motion of total net worth after aggregation is

$$N_{t+1} = \gamma_t\left[(1 - \Gamma_{t-1}(\bar{\omega}_t))R^k_t Q_{\bar{K},t-1}\bar{K}_t\right] + W^{ent}, \tag{A.21}$$

in which $\bar{K}_t$ is the aggregated physical capital.

A.3 Policy Rules and Aggregate Resource Constraint

We consider linearized monetary policy rule

(A.22)

$$R_t - R = \rho_p(R_{t-1} - R) + (1 - \rho_p)\left[\alpha_\pi(\pi_{t+1} - \pi^*_t) + \alpha_{\Delta y}\frac{1}{4}(\Delta y_t - \mu_{z^*})\right] + \frac{1}{400}\sigma_{e,p}\epsilon_{p,t}$$

where ρ_p is the policy smoothing parameter, $\epsilon_{p,t}$ is the monetary policy shock (in annual percentage points), R is the steady-state quarterly interest rate, π^*_t is the inflation target, Δy_t is the quarterly growth in GDP and μ_{z^*} is the corresponding steady state.

The fiscal policy rule of government expenditure follows

$$G^*_t = z^*_t g_t \tag{A.23}$$

with g_t a stationary process, and Y_t/z^*_t converges to a constant in the deterministic

steady state.

Finally, the aggregate resource constraint is given by

$$\begin{aligned} Y_t &= C_t + I_t/(\Upsilon^t \mu_{\Upsilon,t}) + G_t^* \\ &\quad + \mu G_{t-1}(\bar{\omega}_t)(1 + R_t^k) Q_{\bar{K},t-1} \bar{K}_t / P_t + a(u_t)\bar{K}_t \Upsilon^{-t}. \end{aligned} \tag{A.24}$$

Appendix B Solution

B.1 Solution Method

The notation we use within Appendix A is independent of other sections. For $s_t = i$, $s_{t+1} = j$, and $i, j \in \{1, 2\}$, we look for regime-dependent policy functions

$$X_t = T_i(X_{t-1}, \varepsilon_t), \tag{B.1}$$

that solve the system of equations of first-order conditions and constraints

$$0 = E_t \left[\sum_{j=1}^{2} p_{i,j}(\varepsilon_t) f_i(\underbrace{T_j(T_i(X_{t-1}, \varepsilon_t), \varepsilon_{t+1})}_{X_{t+1}}, \underbrace{T_i(X_{t-1}, \varepsilon_t)}_{X_t}, X_{t-1}, \varepsilon_t) \right]. \tag{B.2}$$

We apply the perturbation method proposed by Maih and Waggoner (2018), which features state-dependent policy functions perturbed around the state-dependent steady states $\bar{x}_i$ and perturbation parameter σ in the time-varying transition matrix $p_{i,j}(\varepsilon_t)$. Specifically, Maih and Waggoner (2018) obtain a Taylor series approximation of the regime-dependent policy functions by introducing perturbed policy functions

$$X_t = T_i(X_{t-1}, \sigma, \varepsilon_t), \quad i = 1, 2 \tag{B.3}$$

with perturbation parameter $\sigma \in [0, 1]$ such that

$$T_i\left(X_{t-1}, 1, \varepsilon_t\right) = T_i\left(X_{t-1}, \varepsilon_t\right), \tag{B.4}$$

$$T_i\left(\overline{x}_i, 0, 0\right) = \bar{x}_i. \tag{B.5}$$

The perturbed policy functions solve the system of equations

(B.6)
$$0 = E_t\left[\sum_{j=1,2} p_{i,j}(\sigma,\varepsilon_t) f_i\left(T_j\left(h_i(X_{t-1},\sigma,\varepsilon_t),\sigma,\sigma\varepsilon_{t+1}\right), T_i\left(X_{t-1},\sigma,\varepsilon_t\right), X_{t-1},\varepsilon_t\right)\right],$$

where

(B.7)
$$h_i(X_{t-1},\sigma,\varepsilon_t) = T_i\left(X_{t-1},\sigma,\varepsilon_t\right) + (1-\sigma)\left(\overline{x}_j - T_i\left(\overline{x}_i,0,0\right)\right)$$

(B.8)
$$p_{i,j}(\sigma,\varepsilon_t) = \begin{cases} \sigma p_{i,j}(\varepsilon_t) & \text{for } i \neq j \\ 1-\sigma\left(1-p_{i,i}(\varepsilon_t)\right) & \text{for } i = j \end{cases}$$

Note that the perturbed $h_i(X_{t-1},\sigma,\varepsilon_t)$ and $p_{i,j}(\sigma,\varepsilon_t)$ become the original policy functions to solve and transition probabilities if $\sigma = 1$, and reduces to a tractable system when $\sigma = 0$. Hence, the perturbed system of equations (B.6) reduces to

(B.9)
$$0 = f_i(\bar{x}_i,\bar{x}_i,\bar{x}_i,0),$$

at the steady-state $\bar{x}_i$ when $\sigma = 0, \varepsilon_t = 0$ given (B.5), and is equivalent to (B.2) when $\sigma = 1$. Moreover, the transition probability at the expansion point is an identity matrix. The approximate solutions at expansion points are the state-dependent policy functions assuming the regime is fixed. Finally, the feedback effects disappear in the policy functions by 1-st order solution, and show up in the transition probability functions governing the regime dynamics.

We use the RISE implementation of the solution algorithm by Maih and Waggoner (2018) for computation and estimation purposes.[14].

Appendix C Estimation, Optimization and Filtering Method

This section describes the estimation and filtering procedures of this paper. Additional details of the numerical procedures we implement are available in the Online

[14]RISE is a flexible Matlab toolbox for regime-switching DSGE models. The toolbox is available at https://github.com/jmaih/RISE_toolbox

Appendix.

C.1 Bayesian Estimation

The notation we use within Appendix B is independent of other sections. We perform Bayesian estimation in two steps. The first step is what often referred to as the quasi-Bayesian estimation, in which we resort to numerical optimization and attempt to find

$$\hat{\theta} = \arg\max_{\theta \in \Theta} \Big[\log p(y_{1:T}; \theta) + \log q(\theta) \Big], \tag{C.1}$$

with $q(\theta)$ the prior distribution, and $p(y_{1:T}; \theta)$ the likelihood of θ. The $\hat{\theta}$, if successfully found, is the posterior mode. Although it is generally difficult to obtain $\hat{\theta}$ precisely simply by numerical optimization, the resulting estimate is often a good initial value for the Markov Chain Monte Carlo (MCMC) procedure thereafter. In the second step, we construct MCMC chains of parameters drawn from the posterior distribution, and the posterior mean is calculated from the obtained draws. And we report the 90% Highest Probability Density (HPD) intervals which minimize the ranges on posteriors that cover 90% posterior probability for inference.

The numerical optimization over the posterior surface in the first step entails repeated evaluations of likelihood function $p(y_{1:T}; \theta)$. To this end, we compute the likelihood of each trial point θ taking the following steps:

1. For each trial point θ, solve $X_t = T_i(X_{t-1}, \varepsilon_t; \theta)$.
2. Stack observation equations, regime transitions and solutions to form a state-space representation.
3. Apply Chang et al. (2021) filter to obtain approximated $p(y_{1:T}; \theta)$.

We leave the detail of the optimizer in Appendix C.2 and filtering algorithm in Appendix C.3.

In the second step, we use a Random-Walk Metropolis-Hasting (RWMH) sampler in RISE to draw samples from the posterior distribution $p(\theta|Y_{1:T})$. Specifically, we draw a chain of $\{\theta^i\}$ following steps:

0. Use $\hat{\theta}$ as θ^1.

1. Given $\theta^{i-1}, p(Y|\theta^{i-1})$ and $q(\theta^{i-1})$, draw $\vartheta = \theta^{i-1} + \eta$ with $\eta \sim \mathbb{N}(0, c^2\Sigma_{i-1})$, with the covariance matrix Σ_{i-1} estimated from the sampled draws, and c a scalar.

2. Let $\theta^i = \vartheta$ with probability $\alpha = \min\left\{\frac{p(\vartheta|Y)}{p(\theta^{i-1}|Y)}, 1\right\}$, and $\theta^i = \theta^{i-1}$ otherwise.

In the adaptive setting, the covariance matrix Σ_i computed from the past draws occasionally become numerically singular, with only a few eigenvalues fall inside the neighborhood of zero. We further adjust Σ_i by first obtaining its spectral (eigenvalue) decomposition $U_i\Lambda_i U_i'$, and adding a positive hair amount $\epsilon > 0$ to its eigenvalues to have $\Lambda_i^+ = \Lambda_i + \epsilon I$ where I is an identity matrix of dimension identical to Λ_i. We then use the adjusted covariance $\Sigma_i^+ = U_i\Lambda_i^+ U_i'$ in the RWMH sampler going forward. We choose $\epsilon = 1e-8$ because it appears to us that this small amount is sufficient to handle all the errors we have encountered.

The RWMH algorithm takes a 300,000 burn-in chain and 1,000,000 draws and targets an acceptance rate between .25 and .45 by adjusting the multiplier c in front of Σ_{i-1}. We then thin the collected chain by 100, that is 7,000 accepted draws in total.

C.2 Numerical Optimization

We apply a DIRECT search method with Matlab implementation"Pattern Search", among a collection of alternative methods for its global convergence and superior numerical stability in our application. Alternative methods can generally be divided into local and global methods, as well as derivative-based and derivative-free methods.

Pattern Search is a derivative-free global search method. At iteration i, it evaluates the objective function on grid points round θ_i with distance (mesh size) $d_i = d$ and moves to the point with the highest evaluation in the next iteration, and set $d_{i+1} = 2d$. If it does not find a higher function value, it generates a new set of grid points to evaluate by reducing the distance to $d_{i+1} = d/2$, and stop if $d_{i+1} < \epsilon_{\text{tolerance}}$ that is small. In our application, $\epsilon_{\text{tolerance}} = 1e-5$.

Pattern search is superior to local methods in our exercises because it converges globally provided the objective function has global maximum on a compact support. Its convergence rate is in general slower than derivative-based methods because it

does not take into account the slope information of the objective function. However, it is numerically more stable because the numerical derivatives are often evaluated with non-trivial errors in our problem.

Pattern search, to our experience, is numerically more stable compared to other global methods implemented in Matlab such as particle swarm and simulated annealing because it generates candidate points in a more controlled manner, whereas the alternatives often generate candidates at which the model is unsolvable.

C.3 Filtering Algorithm

We describe the filtering algorithm in this appendix. The readers are referred to the "Endogenous-Switching Kalman Filter" of Chang et al. (2021) (Algorithm 1) for a more extensive exposition. For a $l \times 1$ vector of observable y_t, a $m \times 1$ vector of state variables x_t, and a $k \times 1$ vector predetermined variables z_t, the filtering algorithm considers a state-space model (SSM) of form

$$y_t = D_{s_t} + Z_{s_t} x_t + F_{s_t} z_t + Q_{s_t} u_t, \quad u_t \sim \mathbb{N}(0_{l\times 1}, I_l) \tag{C.2}$$

$$x_t = C_{s_t} + G_{s_t} x_{t-1} + E_{s_t} z_t + R_{s_t} \epsilon_t, \quad \epsilon_t \sim \mathbb{N}(0_{n\times 1}, I_n) \tag{C.3}$$

with s_t specified by

$$w_t = \alpha w_{t-1} + v_t, \quad -1 < \alpha < 1 \tag{C.4}$$

$$s_t = 1 + 1\{w_t \geq \tau\} \tag{C.5}$$

allowing correlation between v_t and ϵ_{t-1} with a $n \times 1$ vector of correlation coefficients ρ. The mapping from our model solution to the SSM above is straightforward.

This filter approximates the likelihood and states using a 'marginalization-collapsing' procedure in the vein of Kim (1994), for an exact filter must track the complete history of $\{s_t\}_{t=1}^T \in \{1, 2\}^T$ which renders the likelihood infeasible to compute for large T. In the marginalization step, the state variables are integrated out with standard Kalman filtering by exploiting the conditional linearity and Gaussianity given the previous state. And in the collapsing step, the history-dependent filtered distributions are approximated by a mixture of two Gaussian distributions.

Appendix D Impulse Response Functions

This section presents a more detailed construction of the impulse response functions we use in the paper.

D.1 Structural Shocks

The h-step ahead impulse response to structural shocks is defined as

$$\mathrm{IR}_x^P(h, e_1^j, s_0) = \mathbb{E}^P(X_h|s_0, X_0, e_1^j, e_{-1}^0) - \mathbb{E}^P(X_h|s_0, X_0, e^0)$$

where $\mathbb{E}^P(\cdot)$ is the expectation with respect to the baseline transition probability matrix P which is subjected to further perturbation by structural shocks through feedback channels. Note that our solution entails regime-dependent policy functions. Specifically, under regime i, for $i = 1, 2$, the solution given state (x, e) is in form of

$$x' = X_i^{ss} + T_i(x - X_i^{ss}) + R_i e$$

in which $X_i^{ss}, i = 1, 2$ are the regime-dependent steady states of X_t, and $(T_i, R_i), i = 1, 2$ are the regime specific solutions solved around the corresponding steady states. Given the regime-dependent policy functions (around regime specific steady states), the h-step forecasts

$$\begin{aligned}
\mathbb{E}^P(X_1|s_0, X_0, e_1^j, e_{-1}^0) &= [X_1^{ss} + T_1(X_0 - X_1^{ss}) + R_1 e_1^j]P(s_1 = 1|s_0) \\
&\quad + [X_2^{ss} + T_2(X_0 - X_2^{ss}) + R_2 e_1^j]P(s_1 = 2|s_0) \\
\mathbb{E}^P(X_1|s_0, X_0, e^0) &= [X_1^{ss} + T_1(X_0 - X_1^{ss})]P(s_1 = 1|s_0) \\
&\quad [X_2^{ss} + T_2(X_0 - X_2^{ss})]P(s_1 = 2|s_0)
\end{aligned}$$

where $P(s_1 = i|s_0), i = 1, 2$ are the baseline transition probabilities given s_0. Therefore, for $h = 1$,

$$\begin{aligned}
\mathrm{IR}_x^P(1, e_1^j, s_0) &= \mathbb{E}^P(X_1|s_0, X_0, e_1^j, e_{-1}^0) - \mathbb{E}^P(X_1|s_0, X_0, e^0) \\
&= [X_1^{ss} + T_1(X_0 - X_1^{ss}) + R_1 e_1^j]P(s_1 = 1|s_0) \\
&\quad + [X_2^{ss} + T_2(X_0 - X_2^{ss}) + R_2 e_1^j]P(s_1 = 2|s_0) \\
&\quad - [X_1^{ss} + T_1(X_0 - X_1^{ss})]P(s_1 = 1|s_0) \\
&\quad - [X_2^{ss} + T_2(X_0 - X_2^{ss})]P(s_1 = 2|s_0) \\
&= \big[R_1 P(s_1 = 1|s_0) + R_2 P(s_1 = 2|s_0)\big] e_1^j
\end{aligned}$$

We can produce the $h-$step impulse responses recursively for $h > 1$. Specifically, for $h \geq 2$,

$$\begin{aligned}
\mathrm{IR}_x^P(h, e_1^j, s_0) &= \mathbb{E}^P(X_h|s_0, X_0, e_1^j, e_{-1}^0) - \mathbb{E}^P(X_h|s_0, X_0, e^0) \\
&= [X_1^{ss} + T_1(\mathbb{E}^P(X_{h-1}|s_0, X_0, e_1^j, e_{-1}^0) - X_1^{ss})]P(s_h = 1|s_0, e_1^j, e_{-1}^0) \\
&\quad + [X_2^{ss} + T_2(\mathbb{E}^P(X_{h-1}|s_0, X_0, e_1^j, e_{-1}^0) - X_2^{ss})]P(s_h = 2|s_0, e_1^j, e_{-1}^0) \\
&\quad - [X_1^{ss} + T_1(\mathbb{E}^P(X_{h-1}|s_0, X_0, e^0) - X_1^{ss})]P(s_h = 1|s_0, e^0) \\
&\quad - [X_2^{ss} + T_2(\mathbb{E}^P(X_{h-1}|s_0, X_0, e^0) - X_2^{ss})]P(s_h = 2|s_0, e^0)
\end{aligned}$$

with the conditional regime probability $P(s_h|s_0, e_1^j, e^0)$ being a function of the shock e_1^j because of the feedback mechanism. Let $P_{1,j}$ be the transition matrix perturbed by shock e_1^j. The h-step conditional regime probabilities under $s_0 = 1$ can be computed as

$$\big(P(s_h = 1|s_0 = 1, e_1^j, e_{-1}^0),\ P(s_h = 2|s_0 = 1, e_1^j, e_{-1}^0)\big) = (1, 0) \times P \times P_{1,j} \times P^{h-2}.$$

in weighting the regime-dependent responses to the structural shocks.

D.2 Uncertainty Shock

With all structural shocks fixed at zero, we consider a one-period perturbation e_1^η of size one to the mean of η_t at $t = 1$. We denote the perturbed transition matrix from

$t = 0$ to $t = 1$ by $P_{0,\eta}$. The impulse response function is defined as

$$\mathrm{IR}_x^P(h, e_1^\eta, s_0) = \mathbb{E}^P(X_h|s_0, X_0, e_1^\eta, e^0) - \mathbb{E}^P(X_h|s_0, X_0, e^0)$$

and is generated recursively for $h = 1, 2, \cdots$. For $h = 1$, we plug in the regime-specific policy function and conditional regime probabilities to have

$$\begin{aligned}
\mathrm{IR}_x^P(1, e_1^\eta, s_0) &= \mathbb{E}^P(X_1|s_0, X_0, e_1^\eta, e^0) - \mathbb{E}^P(X_1|s_0, X_0, e^0) \\
&= [X_1^{ss} + T_1(X_0 - X_1^{ss})]P(s_1 = 1|s_0, e_1^\eta) \\
&\quad + [X_2^{ss} + T_2(X_0 - X_2^{ss})]P(s_1 = 2|s_0, e_1^\eta) \\
&\quad - [X_1^{ss} + T_1(X_0 - X_1^{ss})]P(s_1 = 1|s_0) \\
&\quad - [X_2^{ss} + T_2(X_0 - X_2^{ss})]P(s_1 = 2|s_0) \\
&= [X_1^{ss} + T_1(X_0 - X_1^{ss})] \{P(s_1 = 1|s_0, e_1^\eta) - P(s_1 = 1|s_0)\} \\
&\quad + [X_2^{ss} + T_2(X_0 - X_2^{ss})] \{P(s_1 = 2|s_0, e_1^\eta) - P(s_1 = 2|s_0)\}
\end{aligned}$$

As in the previous subsection, we may recursively obtain impulse responses for $h \geq 2$,

$$\begin{aligned}
\mathrm{IR}_x^P(h, e_1^\eta, s_0) &= \mathbb{E}^P(X_h|s_0, X_0, e_1^\eta, e^0) - \mathbb{E}^P(X_h|s_0, X_0, e^0) \\
&= \left[X_1^{ss} + T_1(\mathbb{E}^P(X_{h-1}|s_0, X_0, e_1^\eta, e^0) - X_1^{ss})\right] P(s_h = 1|s_0, e_1^\eta, e^0) \\
&\quad + \left[X_2^{ss} + T_2(\mathbb{E}^P(X_{h-1}|s_0, X_0, e_1^\eta, e^0) - X_2^{ss})\right] P(s_h = 2|s_0, e_1^\eta, e^0) \\
&\quad - [X_1^{ss} + T_1(\mathbb{E}^P(X_{h-1}|s_0, X_0, e^0) - X_1^{ss})]P(s_h = 1|s_0, e^0) \\
&\quad - [X_2^{ss} + T_2(\mathbb{E}^P(X_{h-1}|s_0, X_0, e^0) - X_2^{ss})]P(s_h = 2|s_0, e^0).
\end{aligned}$$

Note that a perturbation in the η will generate a change in transition probabilities one period earlier than the structural shocks, which leads to h-step conditional regime probabilities under $s_0 = 1$

$$\left(P(s_h = 1|s_0 = 1, e_1^\eta, e^0),\ P(s_h = 2|s_0 = 1, e_1^\eta, e^0)\right) = (1, 0) \times P_{0,\eta} \times P^{h-1}.$$

Appendix E Data Set

We follow CMR closely in constructing and transforming the data set, spanning from 1980Q1 to 2019Q3. In this section, we present the data source for each variable. All data series are obtained from the Federal Reserve Economic Data (FRED) of the Federal Reserve Bank of St. Louis at https://fred.stlouisfed.org. Table 4 and Table 5 provide details of the data series we use to construct the data set in estimation in the alphabetic order. The inflation and relative price of investments are already included in Table 5 are already processed and only require demeaning prior to estimation.

Table 4: Data Source and Description (A-D)

Data Series	Description
A006RD3Q086SBEA	Gross private domestic investment (implicit price deflator), Index 2012=100, Quarterly, Seasonally Adjusted
BAA10YM	Moody's Seasoned Baa Corporate Bond Yield Relative to Yield on 10-Year Treasury Constant Maturity, Percent, Quarterly, Not Seasonally Adjusted
BOGZ1FA234190005Q	Total liabilities Noncorporate farm business, Millions of Dollars, Quarterly, Not Seasonally Adjusted
BOGZ1FL184190005Q	Corporate farm business; total liabilities, Level, Millions of Dollars, Quarterly, Not Seasonally Adjusted
COMPNFB	Nonfarm Business Sector: Compensation Per Hour, Index 2012=100, Quarterly, Seasonally Adjusted
DDURRD3Q086SBEA	Personal consumption expenditures: Durable goods (implicit price deflator), Index 2012=100, Quarterly, Seasonally Adjusted
DFF	Effective Federal Funds Rate, Percent, Quarterly, Not Seasonally Adjusted
DHCERC1Q027SBEA	Personal consumption expenditures: Services: Household consumption expenditures, Billions of Dollars, Quarterly, Seasonally Adjusted Annual Rate
DNDGRD3Q086SBEA	Personal consumption expenditures: Nondurable goods (implicit price deflator), Index 2012=100, Quarterly, Seasonally Adjusted
DSERRD3Q086SBEA	Personal consumption expenditures: Services (implicit price deflator), Index 2012=100, Quarterly, Seasonally Adjusted

Notes: All data series are obtained from FRED of the Federal Reserve Bank of St. Louis at https://fred.stlouisfed.org.

Table 5: Data Source and Description (E-Z)

Data Series	Description
GDP	Gross Domestic Product, Billions of Dollars, Quarterly, Seasonally Adjusted Annual Rate
GDPDEF	Gross Domestic Product: Implicit Price Deflator, Index 2012=100, Quarterly, Seasonally Adjusted
GPDI	Gross Private Domestic Investment, Billions of Dollars, Quarterly, Seasonally Adjusted Annual Rate
HOANBS	Nonfarm Business Sector: Hours of All Persons, Index 2012=100, Quarterly, Seasonally Adjusted
inflation	Log first difference of GDP deflator GDPDEF
LFWA64TTUSQ647S	OECD Working Age Population: Aged 15-64: All Persons for the United States, Persons, Quarterly, Seasonally Adjusted
NCBLL	Nonfinancial corporate business; loans; liability, Level, Millions of Dollars, Quarterly, Not Seasonally Adjusted
NNBLL	Nonfinancial noncorporate business; loans; liability, Level, Millions of Dollars, Quarterly, Not Seasonally Adjusted
PCDG	Personal Consumption Expenditures: Durable Goods, Billions of Dollars, Quarterly, Seasonally Adjusted Annual Rate
PCEND	Personal Consumption Expenditures: Nondurable Goods, Billions of Dollars, Quarterly, Seasonally Adjusted Annual Rate
pinvest	Relative price of investment, log first difference of investment goods deflator A006RD3Q086SBEA over GDP deflator GDPDEF
WILL5000IND	Wilshire 5000 Total Market Index, Index, Quarterly, Not Seasonally Adjusted

Notes: All data series are obtained from FRED of the Federal Reserve Bank of St. Louis at https://fred.stlouisfed.org.